

Analytical Methods for the Detection and Quantification of Trenbolone Acetate Metabolites,
Altrenogest and Related Photoproducts via Liquid Chromatography Tandem Mass Spectrometry

Philip T. Kenyon

A thesis submitted for the partial fulfillment
of the requirements for the degree of

Master of Science in
Civil Engineering

University of Washington

2015

Committee:

Edward Kolodziej

Joel Baker

Program Authorized to Offer Degree:

Civil & Environmental Engineering

©Copyright 2015

Philip Kenyon

University of Washington

Abstract

Analytical Methods for the Detection and Quantification of Trenbolone Acetate Metabolites, Altrenogest and Related Photoproducts via Liquid Chromatography Tandem Mass Spectrometry

Philip T. Kenyon

Chair of Supervisory Committee: Dr. Edward P. Kolodziej

Department of Civil and Environmental Engineering

Photoreaction coupled with liquid chromatography-triple quadrupole tandem mass spectrometry (LC-MS/MS) was used to develop an analytical method for the detection and quantification of trenbolone metabolites, altrenogest, and related photoproducts in water. Target parent analytes were 17 α -trenbolone (17 α -TBOH), 17 β -trenbolone (17 β -TBOH), trendione (TBO), and altrenogest (ALT); target photoproducts were the metastable 5-hydroxy- and 12-hydroxy-photoproducts of 17 α /17 β -TBOH and TBO, and the cyclo-addition and hydroxy-cyclo-addition photoproducts of altrenogest. Photoproducts were generated with a solar simulator reacting trenbolone metabolite (or altrenogest) samples for 6 hrs (>10 half lives). Samples were extracted with C18 solid phase extraction (SPE) cartridges before liquid chromatographic separation with a reverse-phase C18 column with water and methanol mobile phases and ESI+ MS detection. Method detection limits (MDL's) and quantification limits (MQL's) for all compounds were near or below 1 ng L⁻¹ except for 17 β -TBOH photoproducts, which had MDL's <2 ng L⁻¹ and MQL's <4 ng L⁻¹. Matrix suppression was <30% using lake water, and SPE recovery rates were near/above 100%, except for 17 β -TBOH photoproducts, with recoveries >75%. Intra-day relative standard deviations (RSD's) were <30% for TBO and its products, <20% for all others.

Acknowledgements

I would firstly like to thank my adviser, Dr. Ed Kolodziej, for enabling and advising my research at the University of Nevada, Reno, and the University of Washington. I would also like to thank my second committee member, Dr. Joel Baker, for his support and guidance throughout my studies at the University of Washington.

I would like to thank my fellow researchers, Dr. Gerrad D. Jones,, Dr. Bowen Du, Phil Benedetti, Emily Ruskowitz, Tianlin Song, Rachel Weber, Jasmine Miller, Sam Randall, and Alex Gipe, for their advice and contributions to my research.

I also wish to thank my family and friends for their support throughout the duration of my studies, both in Reno and in Tacoma. I would especially like to thank Adrien Goucher, Bryan Kenyon, Linda Kenyon, Patrick Kenyon, and Mark Urlacher.

Lastly, I wish to thank the United States Department of Agriculture and the National Science Foundation for their research grant support, which fueled my research efforts and enabled my success.

Table of Contents

1		
2	List of Figures.....	v
3	List of Tables.....	vii
4	Chapter 1: Introduction	
5	Endocrine-Disrupting Compounds.....	1
6	Growth-Promoter Uses.....	2
7	Progestin Uses.....	4
8	Environmental Fate and Transport of Steroids.....	5
9	Research Objective.....	7
10	Chapter 2: Manuscript	
11	Abstract.....	9
12	1.0 Introduction.....	10
13	2.0 Experimental.....	12
14	2.1 Reagents and Materials.....	12
15	2.2 Sample Preparation.....	13
16	2.3 Photoreaction.....	13
17	2.4 Solid Phase Extraction.....	14
18	2.5 Instrumental Analysis.....	15
19	3.0 Results and Discussion.....	15
20	3.1 Optimization of LC-MS/MS Conditions.....	15
21	3.2 Cationic Adduct Formation.....	17

22	3.3 Chromatography and Spectrometry.....	17
23	3.4 Limits of Detection and Quantification.....	19
24	3.5 Repeatability.....	20
25	3.6 Reversibility.....	20
26	3.7 Recoveries and Matrix Effects.....	22
27	3.8 Archived sample results.....	22
28	4.0 Conclusions.....	23
29	Works Cited.....	24
30	Figures.....	27
31	Tables.....	36
32	Chapter 3: Thiol Adduct Formation	
33	Introduction.....	38
34	Research Objective.....	39
35	Experimental.....	39
36	Deaerating	
37	water.....	41
38	Adduct Formation.....	41
39	Adduct Stability.....	43
40	Conclusions.....	44
41	Works Cited.....	49
42		
43		

44		
45		
46	List of Figures	
47	Figure 1: Trenbolone acetate (TBA) metabolism.....	2
48	Figure 2: Possible adduct formation between 17 β -TBOH and L-cysteine.....	38
49	Figure 3: L-cysteine oxidation to L-cystine in the presence of oxygen.....	40
50	Figure 4: 3-dimensional chromatogram showing L-cysteine (retention time ~2 min, peak	
51	absorbance 220 nm) and 17 β -TBOH (retention time ~11.5 min, peak absorbance 346 nm),	
52	measured via HPLC-DAD.....	42
53	Figure 5: 3D chromatogram showing 17 β -TBOH-L-cysteine adducts (at ~3-3.5 min), with some	
54	residual 17 β -TBOH and L-cysteine. Note the "wall" of background noise at low wavelengths	
55	(~200 nm).....	43
56	Figure 6: Fraction-collected L-cysteine-17 β -TBOH adduct, control (pH=4).....	45
57	Figure 7: Fraction-collected L-cysteine-17 β -TBOH adduct, heated (pH=4).....	46
58	Figure 8: Fraction-collected L-cysteine-17 β -TBOH adduct, basified (pH=13).....	47
59	Figure 9: Fraction-collected L-cysteine-17 β -TBOH adduct, basified (pH=13), then heated.....	48
60	Manuscript Figures	
61	Figure 1: Structures of trenbolone acetate (with carbon numbering), 17 α -trenbolone, 17 β -	
62	trenbolone, trendione, and altrenogest.....	27
63	Figure 2: Chemical structures of the 5-hydroxy and 12-hydroxy photoproducts of 17 α -	
64	trenbolone, 17 β -trenbolone, and trendione, and the cyclo-addition and hydroxy-cyclo-addition	
65	photoproducts of altrenogest.....	28

66 Figure 3: Coupled photohydration-thermal dehydration reversion process of trenbolone acetate
67 metabolites. Reaction shown for 17 α -TBOH, which also applies to 17 β -TBOH, and TBO.....29

68 Figure 4: Photoisomerization of altrenogest to the cyclo-addition photoproduct, and subsequent
69 coupled photohydration-thermal dehydration reversion process of the cyclo-addition and
70 hydroxy-cyclo-addition photoproducts of altrenogest.....29

71 Figure 5: Chromatograms for a.) 17 α -TBOH, b.) 17 β -TBOH, c.) TBO, d.) 17 α -d3-TBOH, and
72 e.) ALT, including retention time (RT), quantitative MRM transition, and most abundant mass-
73 to-charge ratios (m/z) for each. Concentrations for each are 10 ng/L.....30

74 Figure 6: Chromatograms and Spectra for a.) 17 α -TBOH, photo-reacted, not solid phase
75 extracted, b.) 17 α -TBOH, photo-reacted, solid phase extracted, c.) same sample from b.) tested
76 again at T=24hrs, Includes prevalent ions and their retention times (RT), most common mass to
77 charge ratios (m/z), and transition of each chromatogram (note that 271.2->211.2 applies for
78 Figures 6a-d). Figures 6b-c are of the same sample, tested one day apart, where 6b was run
79 immediately, and 6c was run after overnight reversion at room temperature was allowed to take
80 place.....31

81 Figure 7: Chromatograms for a.) 17 β -TBOH, photo-reacted, solid phase extracted, b.) TBO,
82 photo-reacted, solid phase extracted, c.) ALT, photo-reacted, acidified, solid phase extracted, and
83 d.) ALT, photo-reacted, solid phase extracted. Includes prevalent ions and their retention times
84 (RT), most common mass to charge ratios (m/z), and transition of each chromatogram.....32

85 Figure 8: Spectra for a.) 17 α -TBOH, b.) 17 β -TBOH, c.) TBO, and d.) ALT, including retention
86 time (RT) and most abundant mass-to-charge ratios (m/z) for each. Concentrations for each are
87 10 ng/L.....33

88 Figure 9: Spectra for a.) 5-OH-17 α -TBOH, b.) 12-OH-17 β -TBOH, c.) 5-OH-TBO, d.) ALT-
89 CAP, and e.) ALT-CAP-OH, including retention time (RT) and most abundant mass-to-charge
90 ratios (m/z) for each. Concentrations for each are 10 ng/L.....34

91 Figure 10: Indirect photoproduct analysis via acidification or heat, for the primary photoproducts
92 of trenbolone metabolites and ALT-CAP-OH. All concentrations are recovered from 10 ng L⁻¹
93 spikes. Acidified samples were adjusted to pH~2 using HCl after photoreaction. and heated

94 samples were left in a 50° C water bath for 15 hours. 5-OH-, 12-OH- photoproducts and residual
95 parent values are direct photoproduct measurements taken from samples photoreacted without
96 purposeful reversion (left of dashed lines). Heat and acid results were the change in parent
97 concentration after reversion (right of dashed lines).....3

98

99 **List of Tables**

100 Table 1. Commercially available implant formulations currently used by the beef cattle
101 industry.....3

102 Table 2. Summary of log K_{oc} and log K_{ow} for TBA.....6

103 **Manuscript Tables**

104 Table 1: Elution times, Multiple reaction monitoring (MRM) transitions, fragmenter voltages,
105 and collision energies for trenbolone metabolites, altrenogest, and photoproducts. MRM
106 transitions, fragmenter voltages, and collision energies shown are quantitative (confirmatory) for
107 each compound.....36

108 Table 2: Method detection limits (MDL) and quantification limits (MQL), linear regression
109 slopes, intercepts, coefficients of determination (R^2), matrix effects, recoveries from solid
110 phase extraction, relative standard deviations (RSD) at high (10 ng L⁻¹) and low (1 ng L⁻¹) spikes,
111 reversion from photoproducts to parent metabolites, and number of points used in regression, for
112 trenbolone metabolites, altrenogest, and photoproducts. Responses of compounds (3), (4), (5),
113 and (8) in lake water were below detection at tested levels, and were not pursued at higher
114 concentrations since they are minor photoproducts or analogs.....37

115

Chapter 1: Introduction

Endocrine Disrupting Compounds

In recent decades, contaminants which have the capacity to disrupt natural biological processes in animals have become a research priority for identification and control. Once such group of contaminants are labeled "endocrine disrupting compounds" (EDC's), which the National Institute of Environmental Health Services (NIEHS) defines as "chemicals that may interfere with the body's endocrine system and produce adverse developmental, reproductive, neurological, and immune effects in both humans and wildlife" ¹. EDC's are primarily synthetic, and are often described as "contaminants of emerging concern" (CEC's), which the EPA defines as "chemicals [that] are being discovered in water that previously had not been detected or are being detected at levels that may be significantly different than expected" ². EDC's are an increasing concern near agricultural outflows, where high concentrations of steroidal and pharmaceutical metabolites may be present in agricultural runoff, and could potentially affect exposed organisms.

Synthetic EDCs include dioxin-like compounds, polychlorinated biphenyls (PCBs), steroid hormones, pesticides, herbicides, and plasticizers¹. Among steroid hormones, the growth promoter trenbolone (as trenbolone acetate) has been identified as an endocrine active aquatic contaminant³⁻⁶. The ability to detect and quantify these compounds using common analytical methods, such as gas chromatography-mass spectrometry (GC-MS) or liquid chromatography-mass spectrometry (LC-MS) is imperative to understand their ultimate fate and transport within environmental systems.

Growth Promoter Uses

Growth promoters are used in animal agriculture to promote the growth of animals for slaughter. While antibiotics may sometimes be considered growth promoters (they promote growth by minimizing infection), steroidal growth promoters rely upon anabolic properties to improve the conversion of feed into muscle mass. Testosterone is the endogenous androgen, and mimicking its androgenic and anabolic effects is the synthetic androgen trenbolone (see Figure 1). Trenbolone is one of three synthetic hormone growth promoters used widely in the United States, along with the progestin melengestrol acetate and the estrogen zeranol⁷. Trenbolone acetate is applied to cattle as an ear implant, time-releasing trenbolone to the animals and increasing their muscle mass. This results in an important incremental economic effect, with estimates that its use is worth \$1 billion USD per year⁸. Metabolized trenbolone is excreted as the metabolites 17 α -trenbolone (17 α -TBOH, the primary metabolite), 17 β -trenbolone (17 β -TBOH), and trendione (TBO) in urine and manure (see Figure 1)⁹.

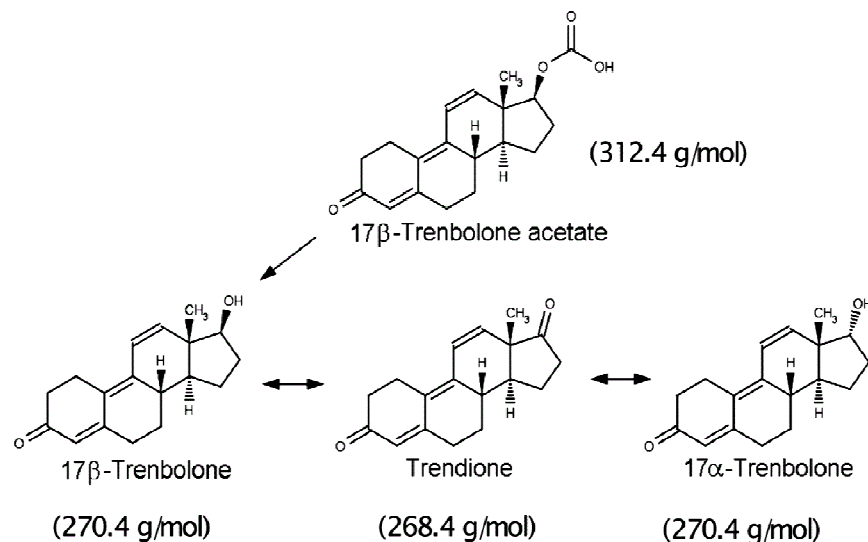


Figure1. Trenbolone acetate (TBA) metabolism. Figure adapted from Khan et al. 2008

Concerns over the environmental implications of metabolites in agricultural runoff reaching surface waters bearing sensitive fish populations have prompted all European countries to ban the use of trenbolone acetate in cattle, however trenbolone is still widely used in the U.S., Australia, and China, among other countries^{10,11}. Table 1 shows commercially available formulations of trenbolone acetate (and other steroids) which are commonly used in the beef cattle industry.

Table 1. Commercially available implant formulations currently used by the beef cattle industry¹².

Hormone	Method of Administration	Dosage	Duration of Effect (days)	Growth Response
Trenbolone Acetate	Pellet implant	200 mg (heifers, cull cows)	60–90	5%–12%
Trenbolone Acetate + Estradiol Benzoate	Pellet implant	200 mg TBA + 28 mg EB (steers, heifers)	90–120	10%–20%
		100 mg TBA + 14 mg EB (steers)	90–120	10%–20%
Trenbolone Acetate + 17 β -Estradiol	Pellet implant	200 mg TBA + 20 mg E (steers, heifers)	90–120	
		120 mg TBA + 24 mg E (steers)	90–120	
		140 mg TBA + 14 mg E	90–120	

		(heifers)		
		80 mg TBA + 16 mg E (steers)	90–120	
		80 mg TBA + 8 mg E (heifers)	90–120	
		40 mg TBA + 8 mg E (steers and heifers grazing pasture)	90–120	
Trenbolone Acetate + 17 β - Estradiol	Pellet implant	200 mg TBA + 40 mg E (steers)	200	
Zeranol	Pellet implant	36 mg zeranol	90–120	10%–15%
		12 mg zeranol	90–120	10%–15%
Melengestrol Acetate	In feed	0.25–0.5 mg/day, PO	As long as it is given	3%–10%
TBA = trenbolone acetate; EB = estradiol benzoate; E = 17 β -estradiol; MGA = melengestrol acetate				

Progestin Uses

Progestins are synthetic progestogens, and are primarily used for hormonal contraception and for use in hormone therapy to treat endometrial hyperplasia. Progestins (like progestogen) suppress ovulation during pregnancy, which is useful both for human use and for veterinary uses. Altrenogest is a progestin, and is administered orally (animal feed) either as an estrus synchronizer, to maintain pregnancy, or to postpone estrus after weaning¹³⁻¹⁶. Swine typically receive 210-360 mg doses of altrenogest over 12-18 days (for horses, 230-400 mg doses over 15 days) for estrus synchronization. Pregnancy maintenance in horses typically involves the

additional dosage of 3000-6000 mg over a 120 day period, with unusual cases allowing for up to 15,000 mg over the entire gestation period of 300 or more days¹⁷⁻¹⁸. Estimating the annual usage of altrenogest is difficult (as is common with veterinary pharmaceuticals due to their industrial-scale use and minimal use regulations), but the most common form, Regu-Mate® has claimed to have sold more than 20 million doses over its 30 year life, at 2.2 mg for every 110 lbs of animal¹⁷. This is particularly important, given that concentrations at sub ng L⁻¹ concentrations of other synthetic progestins, can reduce fecundity in fish¹⁹⁻²¹.

Environmental Fate and Transport of Steroids

Scientific understanding of the fate and transport of many synthetic steroids used as human pharmaceuticals or in animal agriculture is incomplete, making difficult the accurate risk assessment to fish and other organisms from exposure to these compounds. In animal agriculture (specifically cattle) metabolites from implanted steroids (or endogenous steroids) can be detected in manure runoff at 26-370 ng/L²². High mass excretion of steroids via manure and urine (as conjugate steroids), despite dilution, results in these compounds being regularly detected downstream of outflows from animal agriculture. Trenbolone metabolites have been detected downstream at concentrations as high as 10-20 ng/L²³. Natural biodegradation pathways show contrasting evidence between aerobic and anaerobic biodegradation of TBA. Aerobic half lives for TBA metabolites are on the order of 1-5 days^{10,24} while half-lives of TBA metabolites under anaerobic biodegradation show that they are much more stable (half lives of 260 days)²⁵. This suggests that under aerobic conditions (as in a river), TBA metabolites will transform readily, but under anaerobic conditions (as in a manure pile), TBA metabolites are far more likely to remain stable over time.

Additionally, sorption characteristics for trenbolone metabolites indicate that partitioning can be largely affected by soil type and the molecular properties, such as the octanol-water partitioning coefficient. Table 2 shows the organic carbon-water partitioning coefficients and octanol-water partitioning coefficients for the metabolites of trenbolone^{26,27}. From their moderate log K_{ow} values it is clear that TBA metabolites will partition to soil over water, decreasing their aqueous transport rate, but increasing persistence in solids-rich environments. No altrenogest sorption data is available, but computer-modeling based on molecular structure suggests that its log K_{ow} is 3.94²⁸.

Table 2. Summary of log K_{oc} and log K_{ow} for TBA metabolites.

Metabolite	Average \pm SD ^a		
	log K_{oc} ^{b, 26}	log K_{ow} ^{c, 26}	log K_{ow} ^{c, 27}
17 α -trenbolone	2.77 \pm 0.12	2.72 \pm 0.02	2.72
17 β -trenbolone	3.08 \pm 0.10	3.08 \pm 0.03	3.08
Trendione	3.38 \pm 0.19	2.63 \pm 0.05	2.63

^a Standard deviation. ^b Organic-carbon normalized sorption coefficient. ^c Octanol-water partition coefficient.

Concern has grown over the transport of synthetic hormones downstream of animal agriculture due to their high bioactivity at low concentrations. Synthetic hormones are notably more resistant to microbial breakdown than natural hormones, limiting their transformation (and deactivation) pathways, and suggesting that they may be more persistent than natural hormones¹¹. For example, studies demonstrate that trenbolone is stable in manure under

anaerobic conditions for over 260 days¹¹, suggesting that synthetic compounds are of greater concern to ecosystem stability than natural hormones. Data on the biodegradation of altrenogest is unavailable, and environmental degradation of progestins in general is also lacking.

In addition to concerns of the effects of trenbolone metabolites and altrenogest, transformation products can also act as EDCs. Trenbolone metabolites undergo phototransformation with product-to-parent reversion (described later), while altrenogest undergoes a cyclo-addition photoreaction followed with a similar reversible photohydration, a characteristic which could apply to other, structurally similar compounds^{13,29,30}. Additional recent research suggests that trenbolone photoproducts may have their own separate bioactivity of the parent metabolites, meaning that photoreacted metabolites could also impact ecosystems³¹. In the case of the photoproducts of any steroid, methods for their detection and quantification have not yet been developed, leaving a gap in the measurement of steroids, due to the failure to detect photoproducts in addition to parent metabolites.

Research Objective

The critical research objective was to develop an analytical method to simultaneously detect trenbolone metabolites, altrenogest, and related photoproducts, which is sensitive enough to detect all target compounds at environmentally relevant concentrations.

**Analytical Methods for the Detection and Quantification of
Trenbolone Acetate Metabolites and Altrenogest plus
Photoproducts via Liquid Chromatography Tandem Mass
Spectrometry**

Phil Kenyon

Edward Kolodziej

University of Washington

For submission to Journal of Chromatography A

Abstract

Photoreaction coupled with liquid chromatography-triple quadrupole tandem mass spectrometry (LC-MS/MS) was used to develop an analytical method for the detection and quantification of trenbolone metabolites, altrenogest, and related photoproducts in water. Target parent analytes were 17 α -trenbolone (17 α -TBOH), 17 β -trenbolone (17 β -TBOH), trendione (TBO), and altrenogest (ALT); target photoproducts were the metastable 5-hydroxy- and 12-hydroxy- photoproducts of 17 α /17 β -TBOH and TBO, and the cyclo-addition and presumptive 5-hydroxy-cyclo-addition photoproducts of altrenogest. Because they are not commercially available, photoproducts were generated with a solar simulator reacting trenbolone metabolite (or altrenogest) samples for 6 hrs (>10 half lives). Samples were extracted with C18 solid phase extraction (SPE) cartridges before liquid chromatographic separation with a reverse-phase C18 separation column with water/methanol mobile phases and ESI+ MS detection. Method detection limits (MDL's) and quantification limits (MQL's) for all compounds were near or below 1 ng L⁻¹ except for 17 β -TBOH photoproducts, which had MDL's <2 ng L⁻¹ and MQL's <4 ng L⁻¹. Matrix suppression was <30% using lake water, and SPE recovery rates were near/above 100%, except for 17 β -TBOH photoproducts, with recoveries >75%. Intra-day relative standard deviations (RSD's) were <30% for TBO and its products, <20% for all others.

1 **1.0 Introduction**

2 In a resource constrained world with a growing population, increased use of concentrated
3 animal feed operations (CAFO's), a form of intensive industrial agriculture, has resulted in
4 concentrated discharges of pharmaceuticals to natural systems near animal agriculture facilities.
5 Many of these pharmaceuticals are synthetic, and may pose ecological risks through mechanisms
6 of carcinogenicity, teratogenicity, or endocrine disruption [1-7]. Of interest here are steroidal
7 pharmaceuticals used as growth promoters and estrous synchronizers, specifically the
8 metabolites of the synthetic androgen trenbolone acetate (TBA) and the synthetic progestin
9 altrenogest (ALT) (Figure 1). Trenbolone acetate is employed as a growth promoter in beef
10 production, and its use represents significant incremental economic value to the beef industry
11 [8], while altrenogest is used widely as an estrus synchronizer in breeding mares and swine [9-
12 11].

13 The trenbolone metabolites 17 α -trenbolone (17 α -TBOH) and 17 β -trenbolone (17 β -
14 TBOH) have been identified as endocrine disrupting compounds [1-3, 6], and are linked to
15 masculinization and fecundity reduction in fathead minnows and zebrafish [2, 6]. 17 α -TBOH
16 concentrations of 11 ng L⁻¹ significantly reduce fecundity in fathead minnows [3], and
17 concentrations of 9 ng L⁻¹ resulted in male skewed sex ratios in zebrafish [12]. Altrenogest and
18 its photoproducts exhibit potent androgenic effects in *in vitro* cell assays [13]. Endogenous &
19 synthetic steroid hormones have been detected downstream of animal agriculture [8, 14, 15],
20 suggesting that synthetic hormones, such as trenbolone and altrenogest, should be expected to
21 occur in some receiving waters impacted by animal agriculture.

22 In the photic zone, metabolites of trenbolone react rapidly ($k_{\text{obs}}=0.0254 - 0.213 \text{ min}^{-1}$),
23 forming photohydration products [16, 17] (Figure 2). These photoproducts also exhibit thermal
24 dehydration in the dark, reverting to parent structures [18]. Up to 80-90% of 17α -TBOH
25 concentrations can revert to the parent structure from products; reversion is accelerated by higher
26 temperatures and can be nearly instantaneous under strongly acidic or basic conditions (Figure 3)
27 [18]. These mechanisms of reversible transformation can result in higher persistence and
28 increased transport potential of trenbolone metabolites than would be expected based upon initial
29 rates of phototransformation alone [19]. Additionally, evidence suggests that the primary
30 photoproducts of trenbolone metabolites may have bioactivity distinct from that of the parent
31 molecules [20].

32 Under irradiation, altrenogest reacts rapidly ($\sim 30 \text{ s}$) to form a cyclo-addition
33 photoproduct (ALT-CAP) ($k_{\text{obs}}=2.54 \text{ s}^{-1}$), which will then quickly react (3-5 hours) to form a
34 hydrated cyclo-addition photoproduct (ALT-CAP-OH) (Figure 4) [13]. By analogy to trenbolone
35 metabolites, it is very likely that photohydration occurs at carbon-5 in ALT-CAP, although no
36 insights into stereochemistry are possible. The hydrated photoproduct can revert to the cyclo-
37 addition product in the dark, but will not revert back to the altrenogest parent structure [13].
38 These complex dynamics highlight the need for the quantitative and comprehensive analysis of
39 these compounds in aquatic systems, accounting for the dynamic behavior of trenbolone
40 metabolites, altrenogest, and their primary and secondary transformation products.

41 To properly characterize and explore the transport pathways of trenbolone metabolites,
42 altrenogest, and their photoproducts, a method for their detection and quantification is needed.
43 Such methods already exist for trenbolone metabolites [8, 21-23], but not photoproducts; limited
44 options exist for the detection of altrenogest [13], and no method is available for the detection of

45 altrenogest photoproducts. Thus the purpose of this study was to develop an analytical method
46 for the detection and quantification of trenbolone metabolites, altrenogest, and related
47 photoproducts via liquid chromatography tandem mass spectrometry (LC-MS/MS). Additionally,
48 we needed to build a method with sufficient sensitivity and selectivity to detect photoproducts at
49 realistic environmental concentrations, in this case, 1-10 ng L⁻¹ in a complex environmental
50 matrix, typical for systems affected by agricultural runoff [21-23].

51 **2.0 Experimental**

52 *2.1 Reagents and Materials*

53 17β-TBOH was purchased from Shenzhen Shijingu Technology Co. Ltd (Shanghai,
54 China). 17α-TBOH and 17α-16,16,17-d3-TBOH (deuterated internal standard for 17α-TBOH)
55 (17α-d3-TBOH) were purchased from BDG Synthesis (Wellington, New Zealand). Trendione
56 (TBO) was purchased from Steraloids (Newport, Rhode Island). Altrenogest was purchased from
57 Fluka (Sigma Aldrich, St. Louis, MO). LC-MS grade methanol and LC-MS grade water were
58 purchased from Fisher Scientific (Pittsburgh, Pennsylvania).

59 To provide a realistic sample matrix, river water and lake water were used in these
60 studies; river water was collected from the South Fork of the Snoqualmie River (Ollalie State
61 Park, WA, 47.4372° N, 121.6533° W) and used as the primary matrix for method development.
62 This high purity water, near circumneutral (pH=7.2), was used in lieu of LC-MS grade water,
63 which was more acidic (pH=5.5) and would require pH correction (photoproduct reversion is
64 acid catalyzed). Sensitivity decreased due to cationic adduct formation during spectrometry (see
65 section 3.2), so we avoided buffer solutions or pH adjustment to the extent possible. Therefore,
66 this river water source was used for most of our analytical efforts. River water was filtered

67 through a 0.45 μm polyethersulfone (PES) membrane (Fisher Scientific, Pittsburgh,
68 Pennsylvania) to remove particulates. For an organic rich complex matrix representative of
69 agricultural runoff, lake water was collected from Wapato Lake (Tacoma, WA, 47.1952° N,
70 122.4567° W), a highly eutrophic system, to validate the method.

71 *2.2 Sample Preparation*

72 For each metabolite, individual standards (100 ng L⁻¹ to 100 $\mu\text{g L}^{-1}$) were serial dilutions
73 from a stock solution of 10 mg L⁻¹ (metabolite) in methanol, kept at 4° C. Samples for irradiation
74 were either 2 mL HPLC vials (ambered borosilicate glass) with PTFE septa and plastic screw
75 caps, used for injection of samples before/after reaction, or 40 mL samples (clear borosilicate
76 glass), used when solid phase extraction (SPE) was employed. Unless otherwise noted, all data
77 described here was acquired using 40 mL samples concentrated via SPE. All glassware except
78 for transfer pipettes was silanized with 10% (v/v) dichlorodimethylsiloxane in toluene prior to
79 each use. Coelution of metabolites and primary photoproducts in irradiated samples of mixed
80 17 α /17 β -TBOH prevented simultaneous quantification of all primary photoproducts, so parent
81 compounds were irradiated individually to facilitate method development.

82 *2.3 Photoreaction*

83 During photoreaction, samples rested horizontally on a rack in a recirculating 7° C water
84 bath to minimize photoproduct dehydration, such that the water bath elevation did not rise above
85 1/3 to 1/2 the diameter of each vial. The water bath was placed underneath a solar simulator,
86 (EYE Lighting Int. Model # 93510, EYE Lighting, Mentor, OH) that used four high pressure,
87 150 W xenon bulbs (Solarlux 150R, EYE Lighting, Mentor, OH). Per manufacturer
88 specification, the solar simulator was rated to class ABB, simulating sunlight at sea level with

89 low air pollution (rural setting). Trenbolone metabolite samples were irradiated for 6 hours,
90 representing >10 half lives of phototransformation, to maximize photoproduct production [16],
91 and altrenogest samples were irradiated for 1 hour, to maximize the production of the
92 photoproduct ALT-CAP-OH. After irradiation and prior to extraction, internal standard (17 α -d3-
93 TBOH, 2.5 ng L⁻¹) was added to all samples as 40 μ L of a 5 μ g L⁻¹ methanolic standard of 17 α -
94 d3-TBOH to facilitate quantification via isotope dilution techniques.

95 As an alternative to direct photoproduct detection, we also evaluated indirect
96 photoproduct quantification by exploiting the temperature and pH sensitivities of the thermal
97 dehydration reaction (see section 3.6). After irradiation, samples were either placed in a heat bath
98 at 45 $^{\circ}$ C for 15 hours (overnight, to mimic maximum reversion possible naturally), or were
99 acidified with 200 μ L of 1.2 M HCl prior to extraction (final pH ~2.0). Estimates of
100 photoproduct concentration were derived indirectly by comparing observed difference in
101 reversed-photoproduct peak area from unmanipulated trenbolone photoproducts.

102 *2.4 Solid Phase Extraction*

103 Resprep 6 mL C18 SPE cartridges (Restek, Bellefonte, Pennsylvania) (one cartridge per
104 sample) were pre-conditioned with three volumes of methanol added to each cartridge, then
105 allowed to drain and dry. Prior to sample extraction, one volume of water was added, then
106 samples were immediately extracted onto the SPE cartridges under vacuum (4 mL min⁻¹).
107 Samples were eluted with pure methanol using three 1.5 mL aliquots, then blown down to ~1 mL
108 with nitrogen gas from a dry down manifold (Biotage TurboVap LV, Biotage, Charlotte, North
109 Carolina). Samples were then transferred to a 2 mL ambered HPLC vial, and river water was
110 added (50:50, v:v) prior to injection to improve chromatography in LC-MS/MS analysis.

111 2.5 Instrumental analysis

112 An Agilent (Santa Clara, California) 1290 Infinity binary pump liquid chromatograph
113 (LC) coupled with an Agilent 6430 triple quadrupole tandem mass spectrometer (MS/MS) was
114 used for analysis. To minimize reversion and thus maximize photoproduct response, processing
115 time and sample temperatures were minimized to the extent possible. Samples were injected via
116 chilled autosampler tray (4°C) and separated using an Agilent Poroshell 120Å EC C18 column
117 (3.0mm i.d. X 50mm, 2.7µm) preceded by a SecurityGuard Gemini C18 guard column (2.0mm
118 i.d. X 4mm) (Phenomenex, Torrance, California), both at 11°C.

119 Mobile phase (0.2 mL min⁻¹) solutions were A: LC-MS grade water (pH=5.5) and B: LC-
120 MS grade methanol, with the following separation gradient used: 55% B initially, increased to
121 75% over 5 min, increased to 100% B over 3 min, isocratic at 100% B for 3 min, decreased to
122 55% over 1 min, isocratic at 55% B for 5 min, for a total runtime of 17 min. Agilent Jetstream
123 Electrospray Ionization Positive (AJS ESI+) mode was used with 2.5 kV capillary voltage, 1.0
124 kV nozzle voltage, 350°C desolvation gas temp, 400°C sheath gas temp, 12.0 L min⁻¹
125 desolvation and sheath gas flows, 40 psi nebulizer pressure, and 400 V positive multiplier
126 voltage (delta EMV). For all transitions, dwell time was 200 ms and collision cell acceleration
127 voltage was 4 V.

128 3.0 Results and Discussion

129 3.1 Optimization of LC-MS/MS Conditions

130 LC conditions were optimized via serial injection of 100 µg L⁻¹ samples of individual
131 analytes. The LC gradient was adjusted to achieve peak separation of parent metabolites and
132 photoproducts. The method was optimized for 17α-TBOH because it is the predominant

133 metabolite excreted [24]. Photoproduct transitions were determined by photo reacting samples
134 and then scanning for product ions. MS/MS fragmentation conditions were optimized with
135 Agilent Masshunter software (version B.06.00) by varying (in order): fragmenter voltage,
136 collision energy, collision cell accelerator voltage, nebulizer pressure, capillary voltage, and
137 sheath and desolvation gas flows and temperatures; the value corresponding to the best response
138 (highest signal to noise ratio (S/N) and peak area) was selected. The software included an
139 MS/MS auto optimizer, which was used to identify additional confirmatory MS/MS transitions.
140 Auto-optimizer MRM transition and collision energy recommendations were poorly correlated to
141 manually estimated optimization transitions and energies, so these manual optimization
142 transitions and energies were selected to maximize sensitivity. [Table 1](#) shows the optimized
143 retention times, MRM transitions, fragmenter voltages, and collision energies for each of the
144 target steroids, their photoproducts, and the deuterated standard used.

145 $17\alpha/17\beta$ -TBOH had the same precursor mass-to-charge ratio (m/z) of 271.2 Da for their
146 $[M+H]^+$ ions, while their primary photoproducts (5-OH- 17α -TBOH and 12-OH- 17β -TBOH) had
147 an expected precursor m/z of 289.2 Da for their $[M+H]^+$ ions. However, 289.2 Da was never
148 observed via LC-MS/MS, only dehydrated photoproduct ($[M+H-H_2O]^+$) ions with m/z 271.2 Da
149 were observed in LC-MS/MS analysis ([Table 1](#), [Figure 8](#), [Figure 9](#)), consistent with in-source
150 dehydration as previously documented [17]. TBO had a precursor m/z of 269.2 Da, while TBO
151 photoproducts observed (at m/z 269.2 Da) were also dehydrated. ALT and its primary
152 photoproduct (ALT-CAP) both had precursor m/z of 311.2 Da, and the secondary photoproduct
153 (ALT-CAP-OH) had a precursor m/z of 329.2 Da, but only the dehydrated ions ($[M+H-H_2O]^+$)
154 with m/z 311.2 Da were observed for the secondary photoproduct.

155

156 3.2 Cationic Adduct Formation

157 When concentrations were high enough to allow for full scan detection, $[M+H]^+$ parent
158 ions could be resolved from identical mass $[M+H-H_2O]^+$ photoproduct ions by observation of
159 sodium adducts. Spectral analysis revealed that sodium present at the MS ionization source
160 would form an $[M+Na]^+$ adduct with all parent compounds (17α -TBOH, 17β -TBOH, TBO, and
161 ALT), resulting in additions of 22 Da (293.2 Da for $17\alpha/17\beta$ -TBOH, 291.2 for TBO, 333.2 for
162 ALT) ([Figure 8](#)). In photoproducts, sodium replaced a proton on the hydrated molecule $[M+H]^+$
163 (289.2 Da for $17\alpha/17\beta$ -TBOH, 287.2 for TBO, 329.2 for ALT-CAP-OH), resulting in $[M+Na]^+$.
164 However, no in-source dehydration of the photoproduct adducts occurred, resulting in 40 Da
165 additions (compared with protonated photoproduct ions) to detected photoproduct ions (311.2 Da
166 for $17\alpha/17\beta$ -TBOH, 309.2 for TBO, 351.2 for ALT-CAP-OH) ([Figure 9](#)). This pattern was
167 consistently observed for both trenbolone metabolites and altrenogest.

168 Sodium adduct formation also limited method sensitivity, and maximizing method
169 performance required identification and mitigation of adduct sources. Sodium adduct formation
170 was found to be independent of solvent (lake water or river water) and independent of solid-
171 phase extraction. Sodium adduct formation occurred in all samples; the largest single source of
172 sodium contamination was from glassware, but could be minimized via silanization, and all LC
173 lines were purged prior to testing. Sodium adduct formation varied from day to day, and was
174 further aggravated by other instrument user sample matrices.

175 3.3 Chromatography and Spectrometry

176 During analysis of samples that contained similar concentrations of 17α -TBOH and 17β -
177 TBOH photoproducts, the similar polarity of TBA metabolites and photoproducts resulted in

178 peak coelution, rendering true simultaneous multi-residue standard analysis imprecise with these
179 chromatographic conditions. Despite this limitation, which can be addressed by using slower LC
180 gradients at the expense of analytical runtime, the simultaneous occurrence of multiple TBOH
181 metabolite photoproduct groups is unlikely, as 17α -TBOH typically dominates environmental
182 occurrence [24]. [Figure 5](#) shows chromatograms and spectra for 17α -TBOH, 17β -TBOH and
183 TBO metabolites, ALT, and the isotopic standard 17α -d3-TBOH. [Figures 6](#) and [7](#) show the same
184 for TBOH metabolite and ALT photoproducts [13, 25].

185 Given photoproduct instability, several analytical challenges were evident relative to
186 these time scales (days). For example, two peaks were observed in SPE extracts (compounds (4)
187 and (5) in [Table 1](#)) of photo reacted samples of 17α -TBOH that were not observed during direct
188 injection of similar samples (see [Figure 6b](#)). Spectral analysis revealed that the peak at 6.34 min
189 (compound (4)) has similar spectra to the peaks at 6.02 min (5-OH- 17α -TBOH) and 6.53 min
190 (12-OH- 17α -TBOH) and the peak at 7.25 min (compound (5)) has similar spectra to the parent
191 17α -TBOH peak at 6.96 min. These peaks (6.34 min and 7.25 min) are possible analogs of the
192 primary photoproduct (5-OH- 17α -TBOH) and 17α -TBOH respectively, due to the near identical
193 elution time differences from the "new" peaks to their respective parent compounds (0.32
194 minutes +/- 0.03 minutes each). This behavior is not exhibited in dark controls, suggesting that
195 the photoproduct forms an analog in the SPE process, which then reverts to a metabolite analog.
196 Time lapse data (see [Figure 6c](#)) shows that the 5-OH- 17α -TBOH photoproduct, and its potential
197 analog (compounds (2) and (4)), disappear after 1 day (likely due to reversion to parent
198 structures) but 12-OH- 17α -TBOH, 17α -TBOH, and its potential analog (compounds (1), (3), and
199 (5)) all remain. Such observations clearly point to the dynamic nature of photoproduct analysis
200 and highlight the challenges inherent to analysis of complex mixtures.

201 3.4 Limits of Detection and Quantification

202 The method detection limit (MDL) and quantification limit (MQL) were calculated by
203 running matrix blanks (no analyte) 9 times and calculating the average and standard deviation of
204 the background noise, where MDL is defined as the average plus 3 times the standard deviation,
205 and MQL is the average plus 10 times the standard deviation [26-28]. For trenbolone
206 metabolites, altrenogest, and their photoproducts, the MDL's and MQL's were sub ng L^{-1}
207 regardless of sample matrix, with the exception of 12-OH-17 β -TBOH in lake water and 5-OH-
208 17 β -TBOH in river water, both with MDL's $<2 \text{ ng L}^{-1}$ and MQL's $<4 \text{ ng L}^{-1}$ (see Table 2). The
209 photoproducts were more difficult to quantify relative to the parent compounds, due to a.) their
210 reactive nature, and b.) the formation of multiple products, thus reducing available analytical
211 mass (relative to parents).

212 The following assumptions were made to quantify photoproducts: 1.) all metabolite mass
213 is conserved to the photoproducts observed (i.e.; that the sum of photoproduct peak areas at a
214 given concentration equates to the metabolite peak area measured at that concentration); 2.)
215 quantitative transition response of photoproducts is equal to metabolites (i.e. 10 ng L^{-1} of 5-OH-
216 17 α -TBOH measured using m/z 271.2- \rightarrow 211.2 is equal to 10 ng L^{-1} of 17 α -TBOH measured
217 using m/z 271.2- \rightarrow 253.2); and 3.) all photoproducts have the same unit response to detection (i.e.
218 10 ng L^{-1} of 5-OH-17 α -TBOH has the same peak area as 10 ng L^{-1} of 12-OH-17 α -TBOH).

219 Comparing direct injections of parents and photoproducts showed that photoproduct raw
220 peak area response is considerably less than raw parent response (with no change in internal
221 standard response): for 17 α -TBOH, photoproduct response was $57 \pm 7\%$ of parent response; for
222 17 β -TBOH, photoproduct response was $53 \pm 6\%$; for TBO, photoproduct response was $78 \pm$

223 8%; and for ALT, photoproduct response was 11%+/-3% of parent response. [M+Na]⁺ adduct
224 formation is likely to explain some of this difference but regardless, photoproduct peak areas at
225 equal spiked concentrations were reduced from observed parent peak areas, reducing ultimate
226 method sensitivity of photoproducts relative to parents, observable in [Table 2](#).

227 *3.5 Repeatability*

228 Intra-day relative standard deviations (RSD) were calculated ([Table 2](#)) for all compounds
229 in both river water and lake water (n=3 for all), at environmentally relevant concentrations (1
230 ng/L and 10 ng/L, respectively). 17 α -TBOH and 17 β -TBOH metabolites and photoproducts were
231 all below 20% intra-day RSD in river water (40% in lake water), but TBO photoproducts
232 exhibited slightly higher RSD's (RSD <30%) in river water due to lower sensitivity. Intra-day
233 RSD's for ALT and its photoproducts, in both river water and lake water, were all below 20%.
234 Inter-day RSD was based on internal standard response in control samples throughout all
235 experiments, and varied by 69.8% (n=22), largely because detector response was sensitive to use
236 by other researchers and by scheduled maintenance. For this reason, thorough cleaning and
237 purging procedures were employed prior to each instrument use to minimize influence from
238 other users.

239 *3.6 Reversibility*

240 Reversion of trenbolone metabolite photoproducts to parents during sample processing
241 was undesirable, but could be exploited for analysis of ALT-CAP due to its reversible
242 photohydration to ALT-CAP-OH, and because ALT-CAP formation from ALT is irreversible.
243 For trenbolone metabolites and altrenogest, direct injection post-irradiation revealed that
244 complete reaction to photoproducts (and ALT-CAP-OH) consistently occurred, with no

245 observable parent left. However, in samples SPE concentrated prior to analysis, <11% reversion
246 (<30% reversion for ALT-CAP-OH) to parent over 3-5 hours occurred due to sample processing
247 time (see [Table 2](#)), resulting in some loss of analytical sensitivity. Given the dynamic system, we
248 consider the losses during sample processing and analysis acceptable.

249 Indirect quantification of photoproducts was assessed by comparing the difference in
250 peak areas between photoreacted samples and photoreacted samples which were injected then
251 intentionally reverted using heat or acid (quantification by difference) (see [Figure 10](#)). Direct
252 measurement of TBA metabolite photoproducts (5-OH- and 12-OH- columns in [Figure 10](#))
253 resulted in lower total peak area responses than reverted parent measurements (heat and acid
254 columns), but forcing reversion prevents the measurement of individual photoproducts in the
255 case of 17 α -TBOH and 17 β -TBOH. In the case of TBO, reversion was inefficient (heat/acid
256 compared with dark control), resulting in the best measurements coming from direct injection
257 samples. Additionally, comparison of the heat and acid results shows that acid reversion in 17 α -
258 TBOH is the only instance where reversion is ~100%. This complicates indirect analysis for all
259 the other metabolites, as incomplete reversion is an additional variable affecting accurate
260 quantification. Thus accurate quantification of 17 α -TBOH photoproducts via indirect analysis is
261 viable, though limited due to the inability to distinguish individual photoproducts. Indirect
262 photoproduct analysis is not recommended for either 17 β -TBOH or TBO due to limited
263 reversibility.

264 For ALT-CAP-OH, indirect analysis (by quantification of ALT-CAP) was viable when
265 acidification was used, but heat resulted in incomplete reversion (as with trenbolone metabolites)
266 (see [Figure 10](#)). Indirect analysis after acidification resulted in nearly identical response
267 compared to direct analysis of ALT-CAP-OH, and in the acidified sample, no residual ALT-

268 CAP-OH was detected (suggesting ~100% reversion of ALT-CAP-OH to ALT-CAP). What's
269 more, this technique was the only reliable method to directly detect ALT-CAP, as quantification
270 after a short photoreaction period resulted in either residual ALT (unreacted parent) or
271 significant subsequent photohydration to ALT-CAP-OH. It is highly recommended that
272 acidification be used to directly measure ALT-CAP for calibration in the future.

273 *3.7 Recoveries and Matrix Effects*

274 Matrix effects were calculated by comparing internal standard peak areas from (a) direct
275 injection samples with (b) samples of SPE concentrated matrix (no analyte), in which analyte
276 was added immediately before injection [29]. Recovery rates were calculated using 10 ng L⁻¹
277 spikes of analyte, added before extraction. [Table 2](#) shows matrix effects and recoveries for this
278 method for each compound in river water or lake water. River water was found to have an
279 insignificant matrix effect (i.e. peak areas did not change as a result of concentrating river water
280 during SPE), but lake water concentration resulted in a 10-30% decrease in response (matrix
281 suppression). Recovery rates (n=3) were above 103-125% for 17 α -TBOH and its photoproducts,
282 105-119% for 17 β -TBOH and 75-93% for its photoproducts, 95-116% for TBO and its
283 photoproducts, and 88-116% for ALT and its photoproducts.

284 *3.8 Archived sample results*

285 Archived samples were provided from the United States Geological Survey (USGS),
286 dated 06/2009 to 04/2011, collected from a variety of sources: feces, lagoon solids, lagoon
287 liquid, barn flush solids, barn flush liquid, and urine. Samples were previously concentrated via
288 solid-phase extraction, and when received were dehydrated. Samples were reconstituted in 200
289 μ L of methanol and 100 μ L of nanopure water, then tested for trenbolone metabolites,

290 altrenogest, and related photoproducts, however, no target analytes were detected. Due to the
291 dehydrated nature of the samples when received, it is unknown whether any target analytes were
292 present when sampling occurred and subsequently transformed during storage. Attempts to
293 analyze more recent samples which might contain target analytes are recommended for future
294 analysis.

295 **4.0 Conclusions**

296 A multi-residue LC-MS/MS method coupled with photoreaction and SPE concentration
297 was developed and optimized for the detection of trenbolone metabolites, altrenogest, and their
298 related photoproducts. Initial efforts utilized filtered, circumneutral-pH river water, followed by
299 method validation using the more complex matrix of Wapato Lake water to better mimic
300 receiving waters. This method allowed for consistent detection of trenbolone metabolites,
301 altrenogest, and related photoproducts, relying on a short sample preparation time (3 hours) to
302 minimize product-to-parent reversion, and minimized variability (intra-day RSD <20% for 17 α -
303 TBOH photoproducts). Using 1-10 ng L⁻¹ spike concentrations, most recoveries were 90-120%,
304 and limited matrix suppression (<30%) was observed. Critically, method detection and
305 quantification limits were at or below environmentally relevant concentrations (1-10 ng L⁻¹
306 concentrations) for all metabolites and all photoproducts, and calibration curves were linear
307 across ~3 orders of magnitude. Further sensitivity and selectivity could be achieved with the use
308 of a dedicated instrument to minimize inter-day variability and sodium adduct formation, or via
309 the use of a longer LC gradient to improve separation of metabolite photoproducts, (at the
310 expense of longer runtime and increased reversion potential). This method could be applied to
311 water samples affected by agricultural runoff in lieu of existing detection methods for trenbolone

312 metabolites and altrenogest, while also allowing for detection of their photoproducts, potentially
313 critical aspects of environmental risk assessment of these agricultural pharmaceuticals.

314

315

316

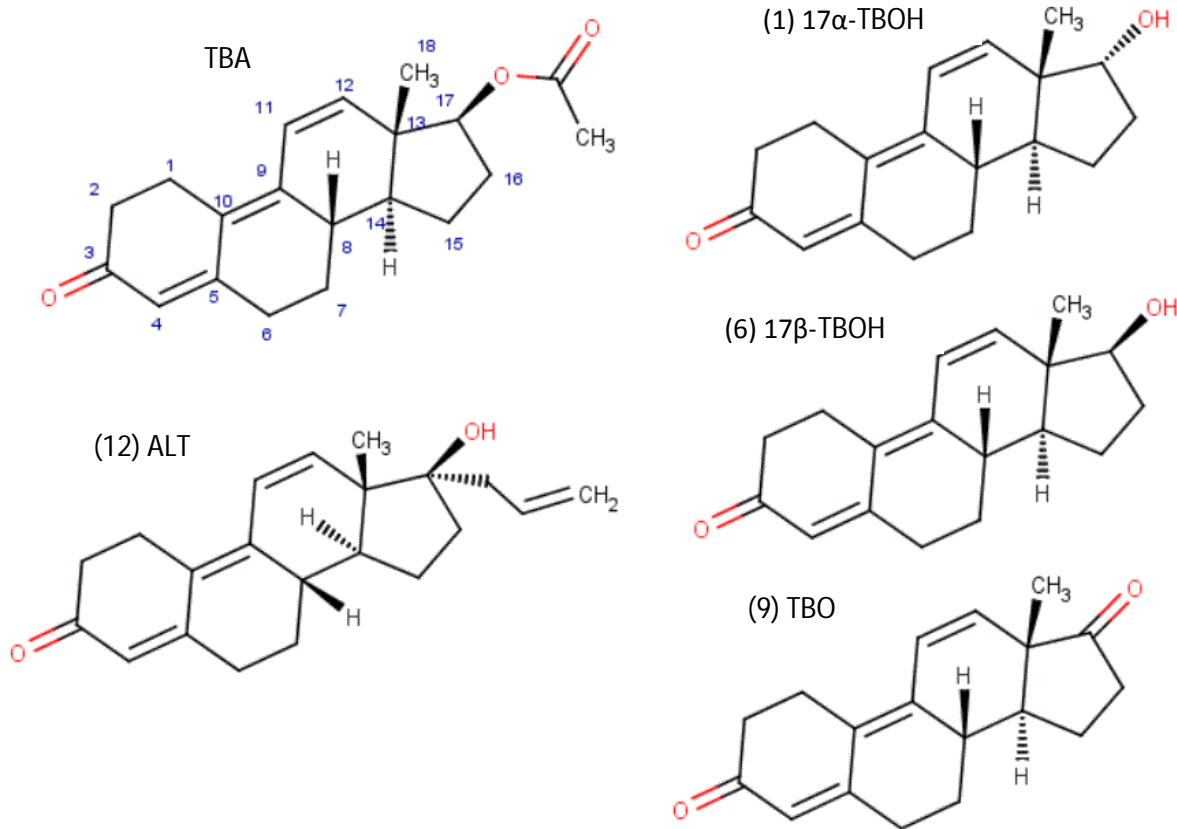
317 **Works Cited**

- 318 1. Howell, W. M.; Black, D. A.; Bortone, S. A., Abnormal Expression of Secondary Sex
319 Characters in a Population of Mosquitofish, *Gambusia affinis holbrooki*: Evidence for
320 Environmentally Induced Masculinization. *Copeia*. (1980), 676-681.
- 321 2. Sone, K.; M. H.; Itamoto, M.; Katsu, Y.; Watanabe, H.; Urushitani, H.; Tooi, O.;
322 Guillette Jr., L. J.; Taisen, I. Effects of an androgenic growth promoter 17 β trenbolone on
323 masculinization of Mosquitofish (*Gambusia affinis affinis*). *Gen. Comp. Endocrinol.* (2005) 143,
324 151-160.
- 325 3. Jensen, K. M.; E. A. M.; Kahl, M. D.; Ankley, G. T. Effects of the Feedlot Contaminant
326 17 α Trenbolone on Reproductive Endocrinology of the Fathead Minnow. *Environ. Sci. Technol.*
327 (2006) 40, 3112-3117.
- 328 4. Duguet, J. P.; Bruchet, A.; Mallevalle, J. Pharmaceuticals and endocrine disruptors in the
329 water cycle. *IWA Yearb.* (2004) 41-46.
- 330 5. Orlando, E. F.; Kolok, A. S.; Binzcik, G. A.; Gates, J. L.; Horton, M. K.; Lambright, C.
331 S.; Gray, L. E.; Soto, A. M.; Guillette, L. J. Endocrine disrupting effects of cattle feedlot effluent
332 on an aquatic sentinel species, the fathead minnow. *Environ. Health Perspect.* (2004) 112, 353-
333 358.
- 334 6. Seki, M., S. Fujishima, T. Nozaka, M. Maeda & K. Kobayashi. Comparison of response
335 to 17 beta estradiol and 17 beta trenbolone among three small fish species. *Environ. Toxicol.*
336 *Chem.* (2006) 25, 2742-2752.
- 337 7. Kumar, V.; Johnson, A.C.; Trubiroha, A.; Tumova, J.; Ihara, M.; Grabic, R.; Kloas, W.;
338 Tanaka, H.; Kroupova, H.K. The challenge presented by progestins in ecotoxicological research:
339 A critical review. *Environ. Sci. Technol.* (2015), 49, 2625-2638.
- 340 8. Khan, B.; Lee, L. S., Estrogens and synthetic androgens in manure slurry from trenbolone
341 acetate/estradiol implanted cattle and in waste receiving lagoons used for irrigation.
342 *Chemosphere* (2012), 89, 1443-1449.
- 343 9. Squires, E.L.; Heesemann, C.P.; Webel, S.K.; Shideler, R.K.; Voss, J.L. Relationship of
344 altrenogest to ovarian activity, hormone concentrations and fertility of mares. *J. Anim. Sci.*
345 (1983), 56, 901-910.
- 346 10. van Leeuwen, J.J.J.; Williams, S.I.; Martens, M.R.T.M.; Jourquin, J.; Driancourt, M.A.;
347 Kemp, B.; Soede, N.M. The effect of post weaning altrenogest treatments of primiparous sows
348 on follicular development, pregnancy rates, and litter sizes. *J. Anim. Sci.* (2011), 89, 397-403.
- 349 11. Willmann, C.; Schuler, G.; Hoffmann, B.; Parvizi, N.; Aurich, C. Effects of age and
350 altrenogest treatment on conceptus development and secretion of LH, progesterone, and eCG in
351 early-pregnant mares. *Theriogenology*. (2011), 75, 421-428.

- 352 12. Morthorst, J.E.; Holbech, H.; Bjerregaard, P. Trenbolone causes irreversible
353 masculinization of zebrafish at environmentally relevant concentrations. *Aquat. Toxicol.* (2010).
354 98(4), 336-343.
- 355 13. Wammer, K. H.; Anderson, K. C.; Erickson, P. R.; Kliegman, S.; Moffatt, M.; Berg, S.
356 M.; Heitzman, J. A.; McNeill, K.; Martinovic-Weigelt, D.; Cwiertny, D. M.; Kolodziej, E. P.
357 Environmental photochemistry of altrenogest: photoisomerization to a bioactive product with
358 increased environmental persistence via reversible photohydration. In review.
- 359 14. Kolodziej, E. P. & D. L. Sedlak (2007) Rangeland grazing as a source of steroid
360 hormones to surface waters. *Environ. Sci. Technol.* (2007), 41, 3514-3520.
- 361 15. Gall, H. E.; Sassman, S. A.; Lee, L. S.; Jafvert, C. T. Hormone discharges from a
362 midwest tile-drained agroecosystem receiving animal wastes. *Environ. Sci. Technol.* (2011).
363 45(20), 8755-8764.
- 364 16. Qu, S.; Kolodziej, E. P.; Cwiertny, D. M., Phototransformation Rates and Mechanisms
365 for Synthetic Hormone Growth Promoters Used in Animal Agriculture. *Environ. Sci. Technol.*
366 (2012), 46, 13202-13211.
- 367 17. Kolodziej, E. P.; Qu, S.; Forsgren, K. L.; Long, S. A.; Gloer, J. B.; Jones, G. D.; Schlenk,
368 D.; Baltrusaitis, J.; Cwiertny, D. M. Identification and Environmental Implications of Photo
369 Transformation Products of Trenbolone Acetate Metabolites. *Environ. Sci. Technol.* (2013), 47,
370 5031-5041.
- 371 18. Qu, S.; Kolodziej, E. P.; Long, S. A.; Gloer, J. B.; Patterson, E. V.; Baltrusaitis, J.;
372 Jones, G. D.; Benchetler, P. V.; Cole, E. A.; Kimbrough, K. C.; Tarnoff, M. D.; Cwiertny, D. M.
373 Product to Parent Reversion of Trenbolone: Unrecognized Risks for Endocrine Disruption. *Sci.*
374 (2013), 342, 347-351.
- 375 19. Ward, A. S.; Cwiertny, D. M.; Kolodziej, E. P.; Brehm, C. C. Coupled reversion and
376 stream hyporheic exchange processes increase environmental persistence of trenbolone
377 metabolites. *Nat. Commun.* (2015), 6:7067, 1-10.
- 378 20. Forsgren, K. L.; Qu, S.; Lavado, R.; Cwiertny, D.; Schlenk, D. Trenbolone acetate
379 metabolites promote ovarian growth and development in adult Japanese medaka (*Oryzias*
380 *Latipes*). *Gen. Comp. Endocrinol.* (2014), 202, 1-7.
- 381 21. Khan, B.; Lee, L. S.; Sassman, S. A. Degradation of Synthetic Androgens 17 α and 17 β
382 Trenbolone and Trendione in Agricultural Soils. *Environ. Sci. Technol.* (2008), 42, 3570-3574.
- 383 22. Webster, J. P.; Kover, S. C.; Bryson, R. J.; Harter, T.; Mansell, D. S.; Sedlak, D. L.;
384 Kolodziej, E. P. Occurrence of Trenbolone Acetate Metabolites in Simulated Confined Animal
385 Feeding Operation (CAFO) Runoff. *Environ. Sci. Technol.* (2012), 46, 3803-3810.
- 386 23. Durhan, E. J.; Lambright, C. S.; Makynen, E. A.; Lazorchak, J.; Hartig, P. C.; Wilson, V.
387 S.; Gray, L. E.; Ankley, G. T. Identification of metabolites of trenbolone acetate in androgenic
388 runoff from a beef feedlot. *Environ. Health Perspect.* (2006), 114, 65-68.

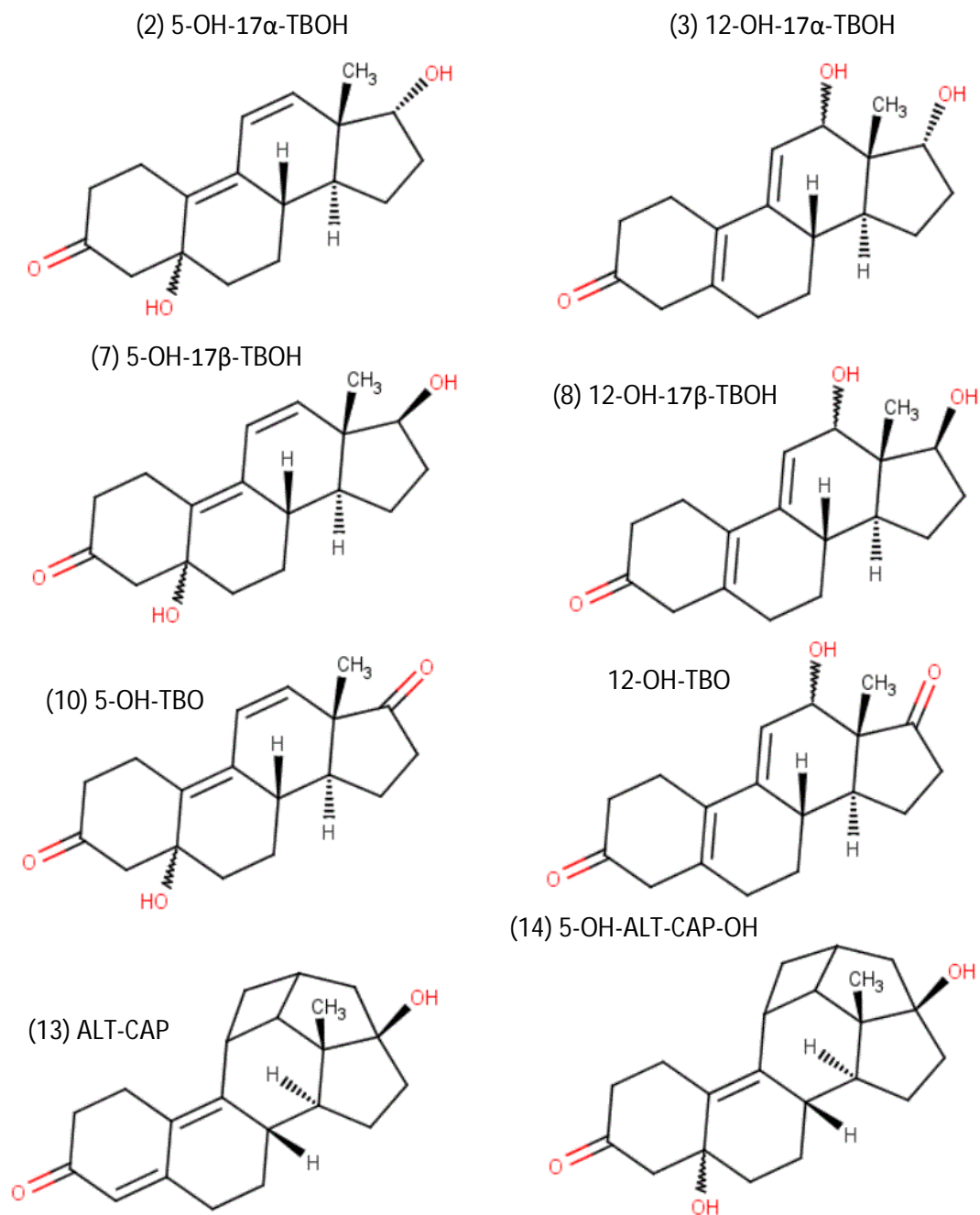
- 389 24. Jones, G. D.; Benchetler, P. V.; Tate, K. W.; Kolodziej, E. P. Mass balance approaches to
390 characterizing the leaching potential of trenbolone acetate metabolites in agro-ecosystems.
391 *Environ. Sci. Technol.* (2014), 48(7), 3715-3723.
- 392 25. Baltrusaitis, J.; Patterson, E. V.; O'Connor, M.; Qu, S.; Kolodziej, E. P.; Cwiertny, D.
393 Reversible photohydration of trenbolone acetate metabolites: mechanistic understanding of
394 product to parent reversion through complementary experimental and theoretical approaches. *J.*
395 *Am. Chem. Soc.* (2015), In review.
- 396 26. Farre, M.; Pico, Y.; Barcelo, D. Application of ultra-high pressure liquid chromatography
397 linear ion-trap orbitrap to qualitative and quantitative assessment of pesticide residues. *J. Chrom.*
398 *A.* (2014), 1328, 66-79.
- 399 27. Mou, R.; Chen, M.; Cao, Z.; Zhu, Z. Simultaneous determination of triazine herbicides in
400 rice by high-performance liquid chromatography coupled with high resolution and high mass
401 accuracy hybrid linear ion trap-orbitrap mass spectrometry. *Analytica Chimica Acta.* (2011),
402 706(1), 149-156.
- 403 28. Fernandez-Arauzo, L.; Pimentel-Trapero, M.; Hernandez-Carrasquilla, M. Simultaneous
404 determination of resorcylic acid lactones, β and α trenbolone and stilbenes in bovine urine by
405 UHPLC/MS/MS. *J. Chrom. B.* (2014), 973, 89-96.
- 406 29. Gosetti, F.; Mazzucco, E.; Zampieri, D.; Gennaro, M. C. Signal suppression/enhancement
407 in high-performance liquid chromatography tandem mass spectrometry. *J. Chrom A.* (2010).
408 1217(25), 3929-3937.
- 409

410 **List of Figures**



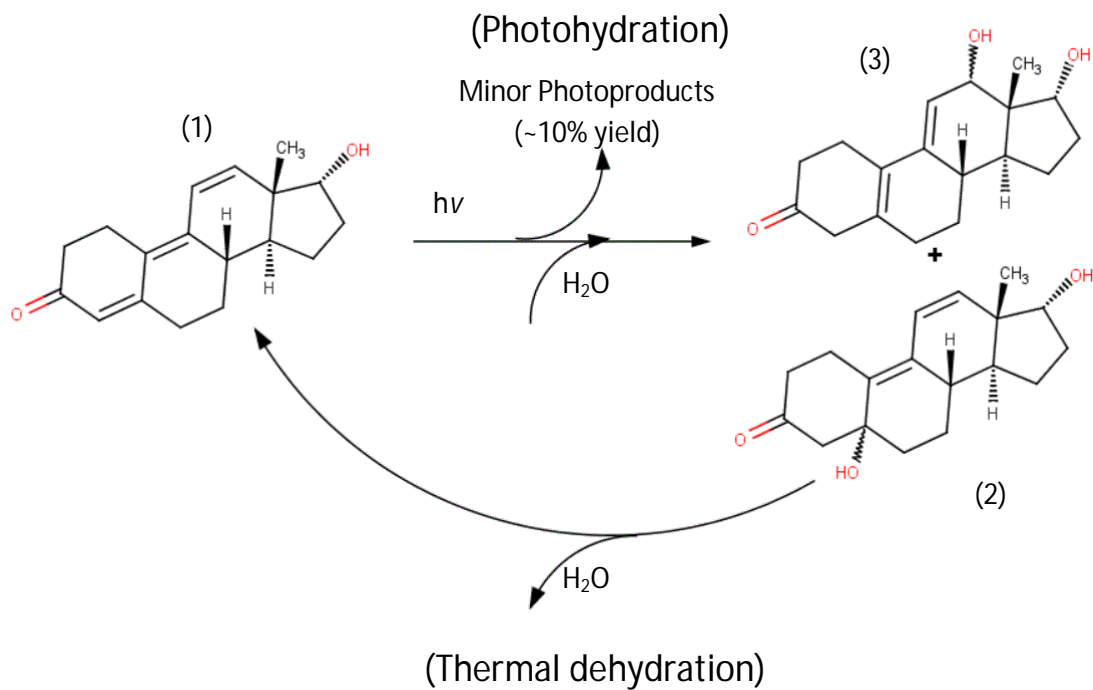
411

412 **Figure 1:** Structures of trenbolone acetate (with carbon numbering), 17 α -trenbolone, 17 β -
413 trenbolone, trendione, and altrenogest.



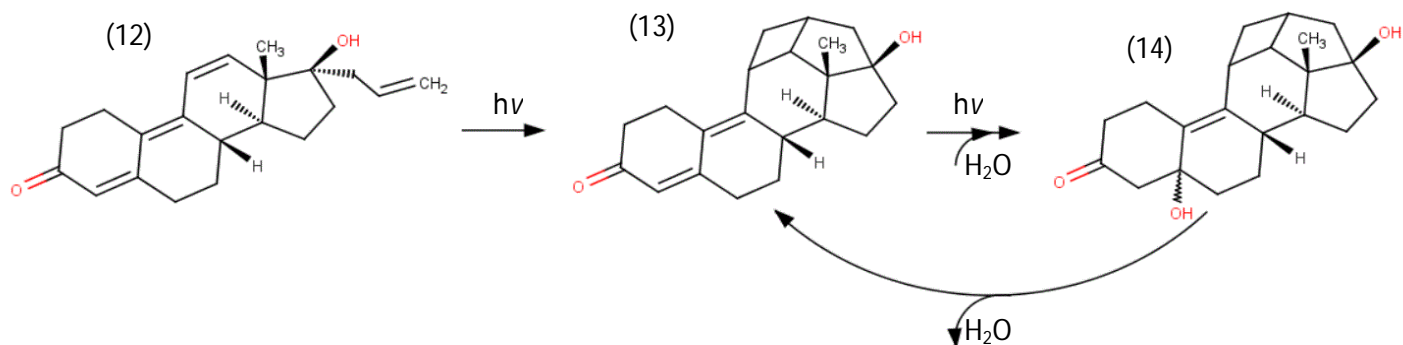
414

415 **Figure 2:** Chemical structures of the 5-hydroxy and 12-hydroxy photoproducts of 17 α -
 416 trenbolone, 17 β -trenbolone, and trendione, and the cyclo-addition and hydroxy-cyclo-addition
 417 photoproducts of altrenogest.



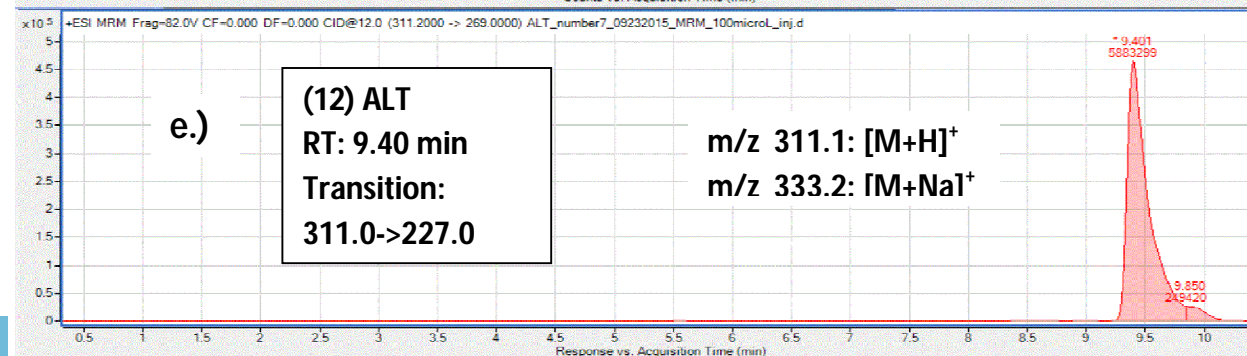
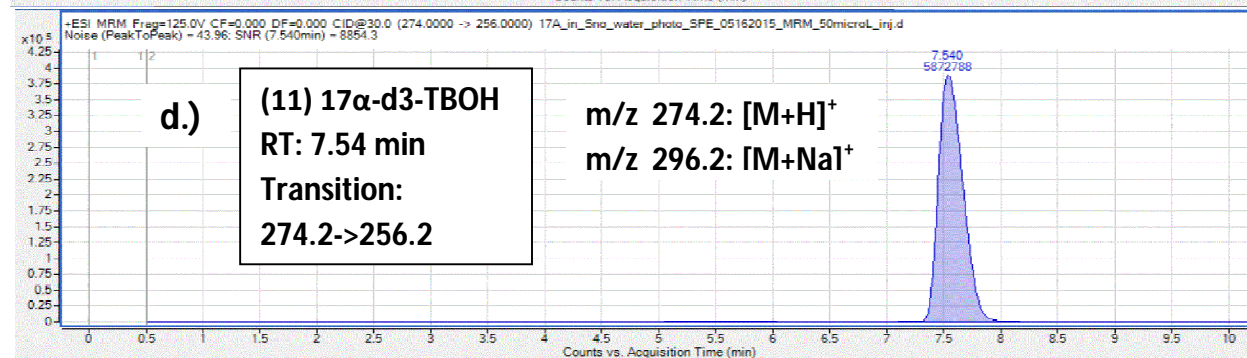
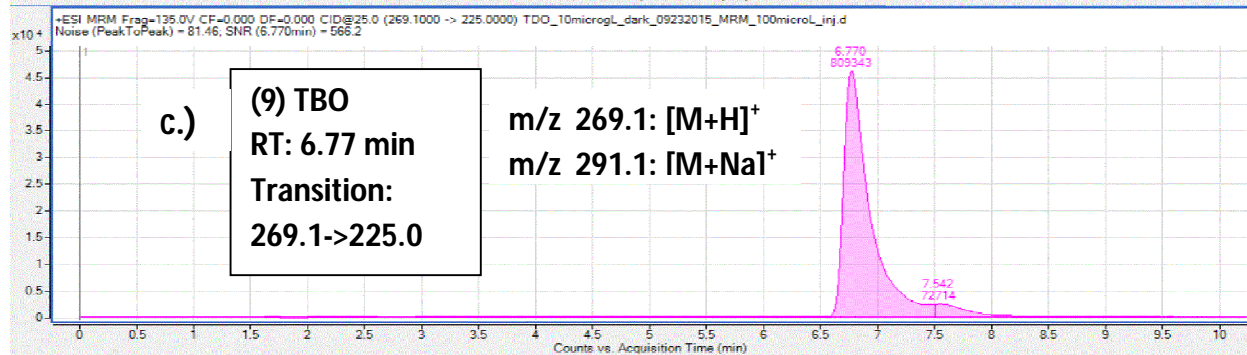
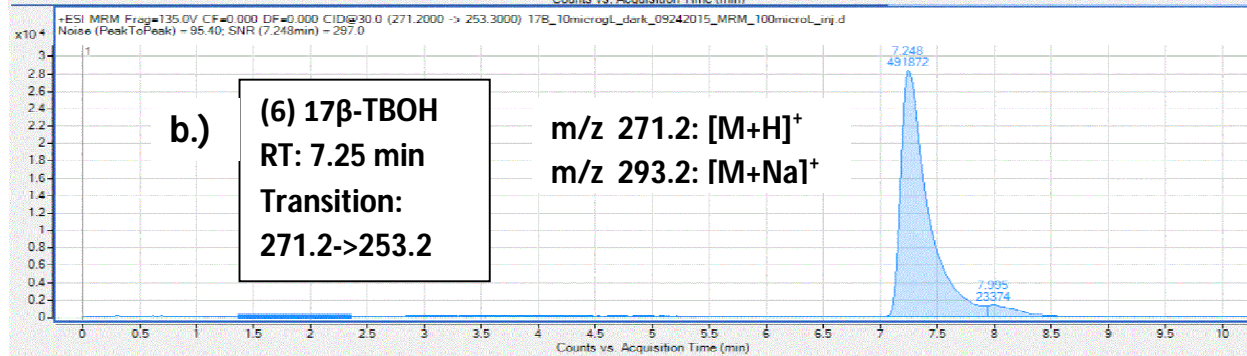
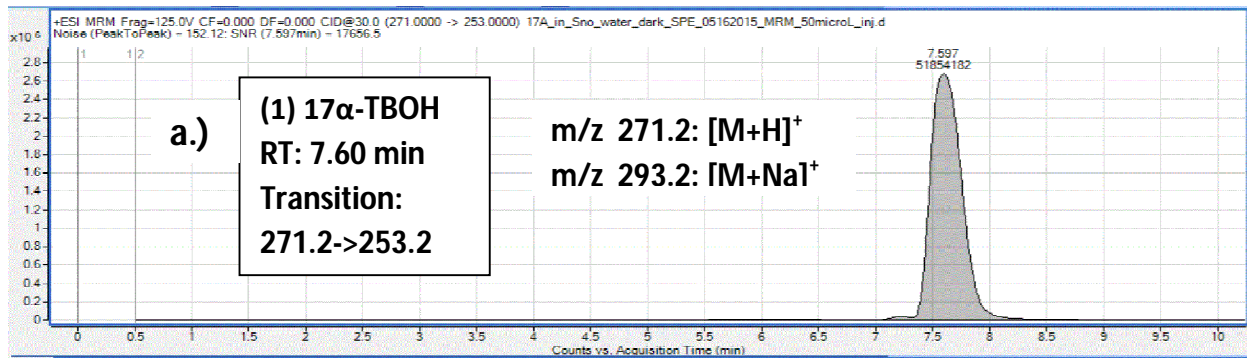
418

419 **Figure 3:** Coupled photohydration-thermal dehydration reversion process of trenbolone acetate
 420 metabolites. Reaction shown for 17 α -TBOH, which also applies to 17 β -TBOH, and TBO [17].

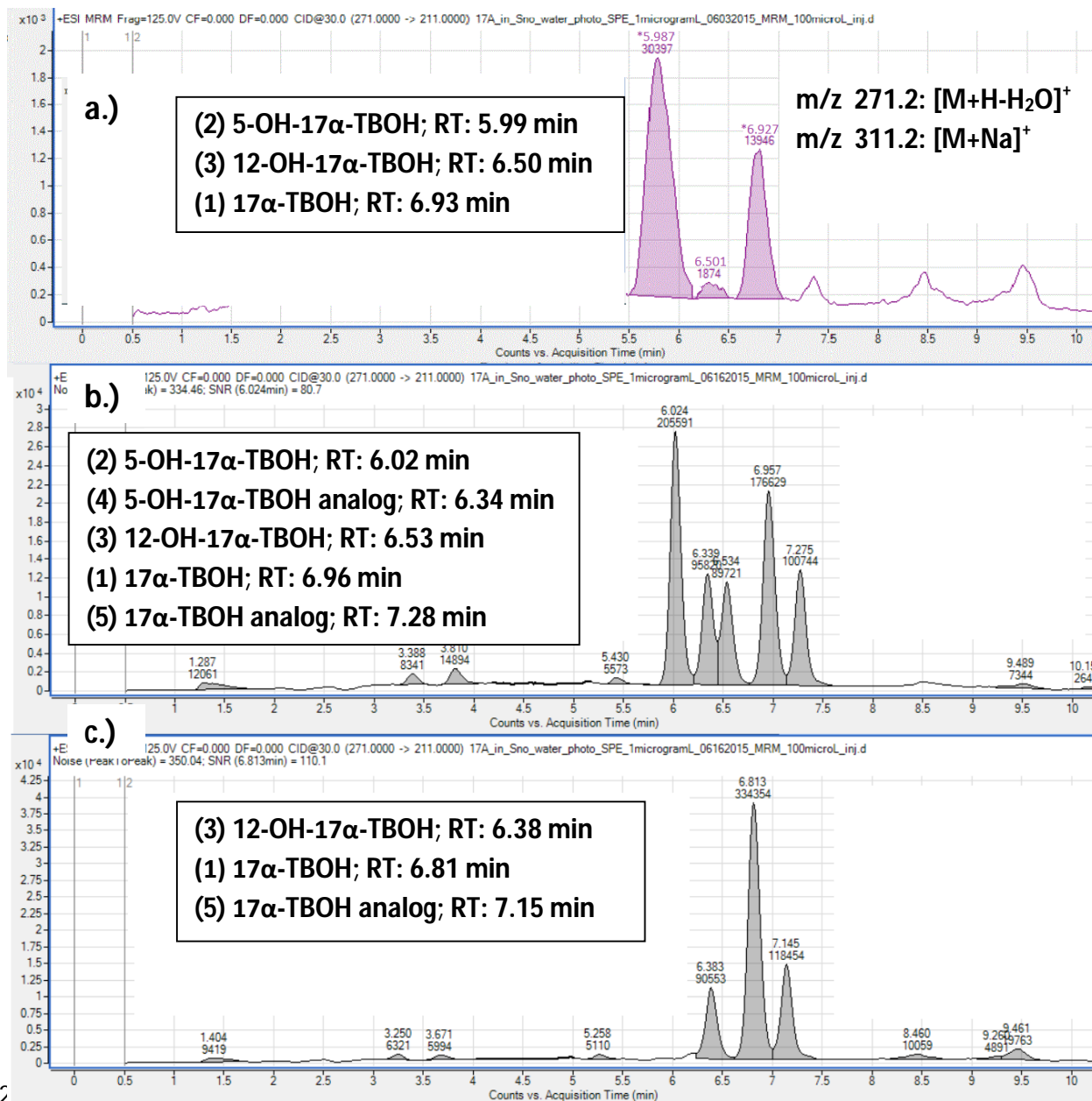


42

422 **Figure 4:** Photoisomerization of altrenogest to the cyclo-addition photoproduct, and subsequent
 423 coupled photohydration-thermal dehydration reversion process of the cyclo-addition and
 424 hydroxy-cyclo-addition photoproducts of altrenogest [13].

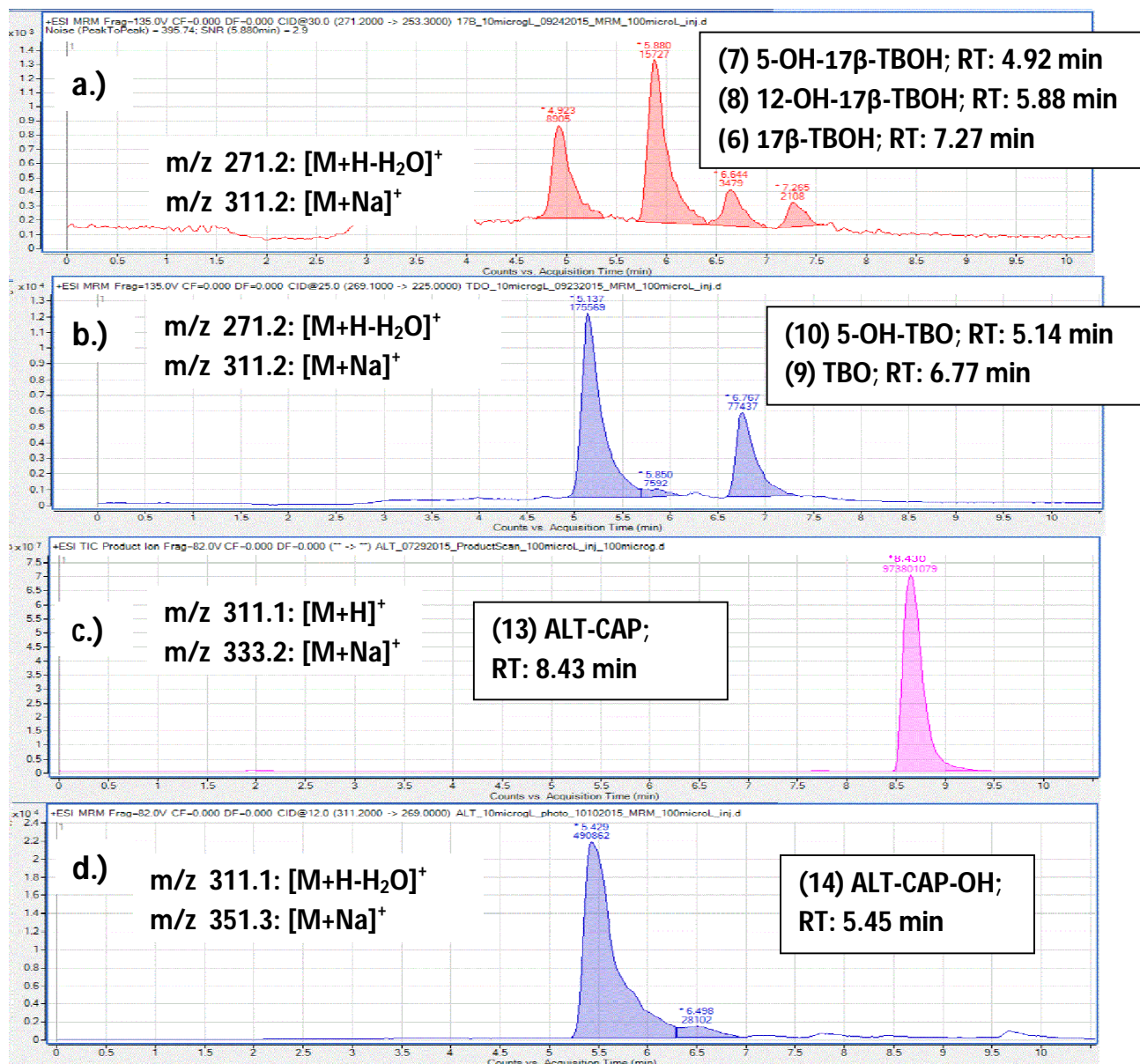


426 **Figure 5:** Chromatograms for a.), 17 α -TBOH, b.) 17 β -TBOH, c.) TBO, d.) 17 α -d3-TBOH, and
 427 e.) ALT, including retention time (RT), quantitative MRM transition, and most abundant mass-
 428 to-charge ratios (m/z) for each. Concentrations for each are 10 ng/L.



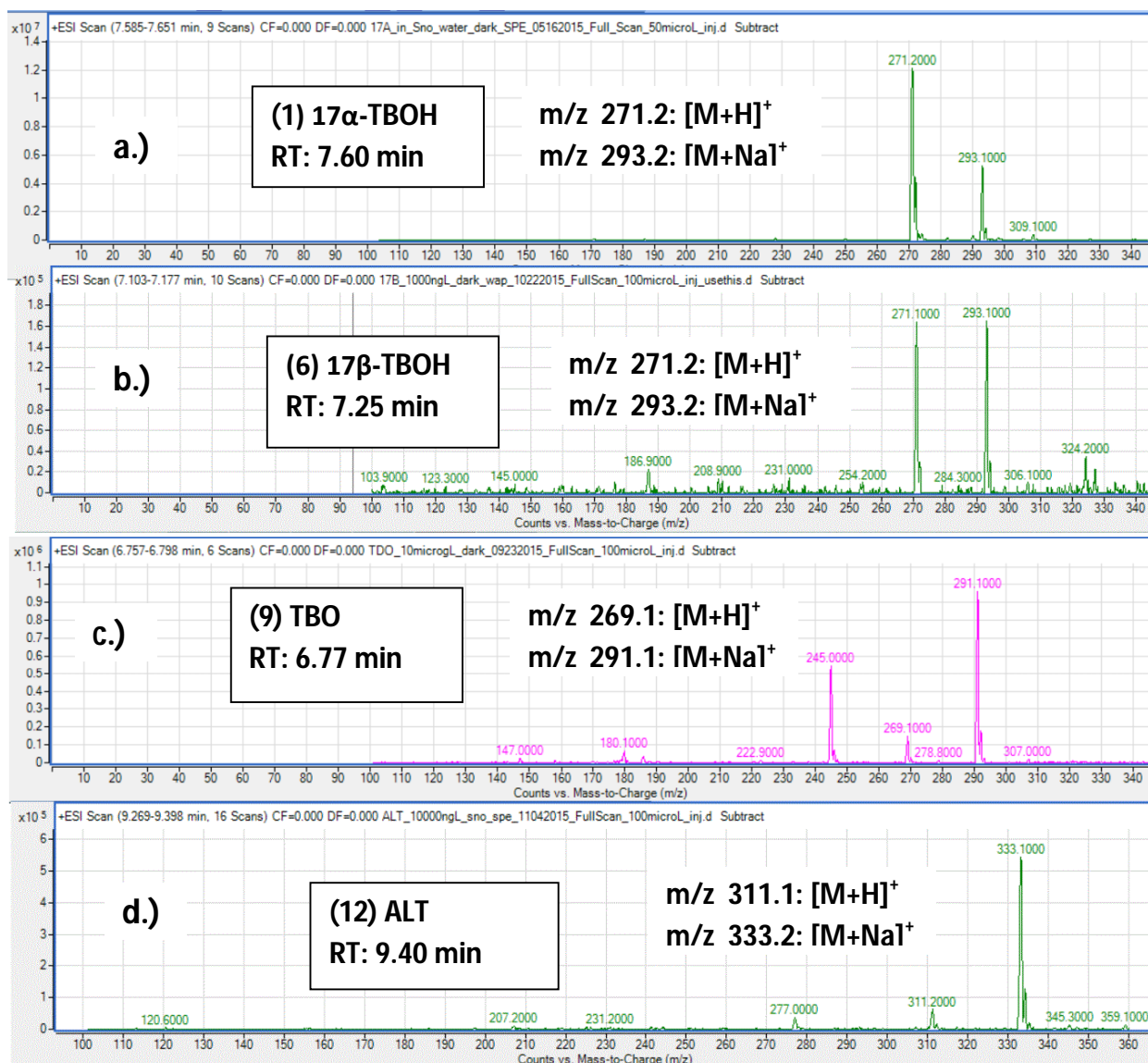
429 **Figure 6:** Chromatograms and Spectra for a.) 17 α -TBOH, photo-reacted, not solid phase
 430 extracted, b.) 17 α -TBOH, photo-reacted, solid phase extracted, c.) same sample from b.) tested
 431

432 again at T=24hrs, Includes prevalent ions and their retention times (RT), most common mass to
 433 charge ratios (m/z), and transition of each chromatogram (note that 271.2->211.2 applies for
 434 Figures 6a-c). Figures 6b-c are of the same sample, tested one day apart, where 6b was run
 435 immediately, and 6c was run after overnight reversion at room temperature was allowed to take
 436 place.



437

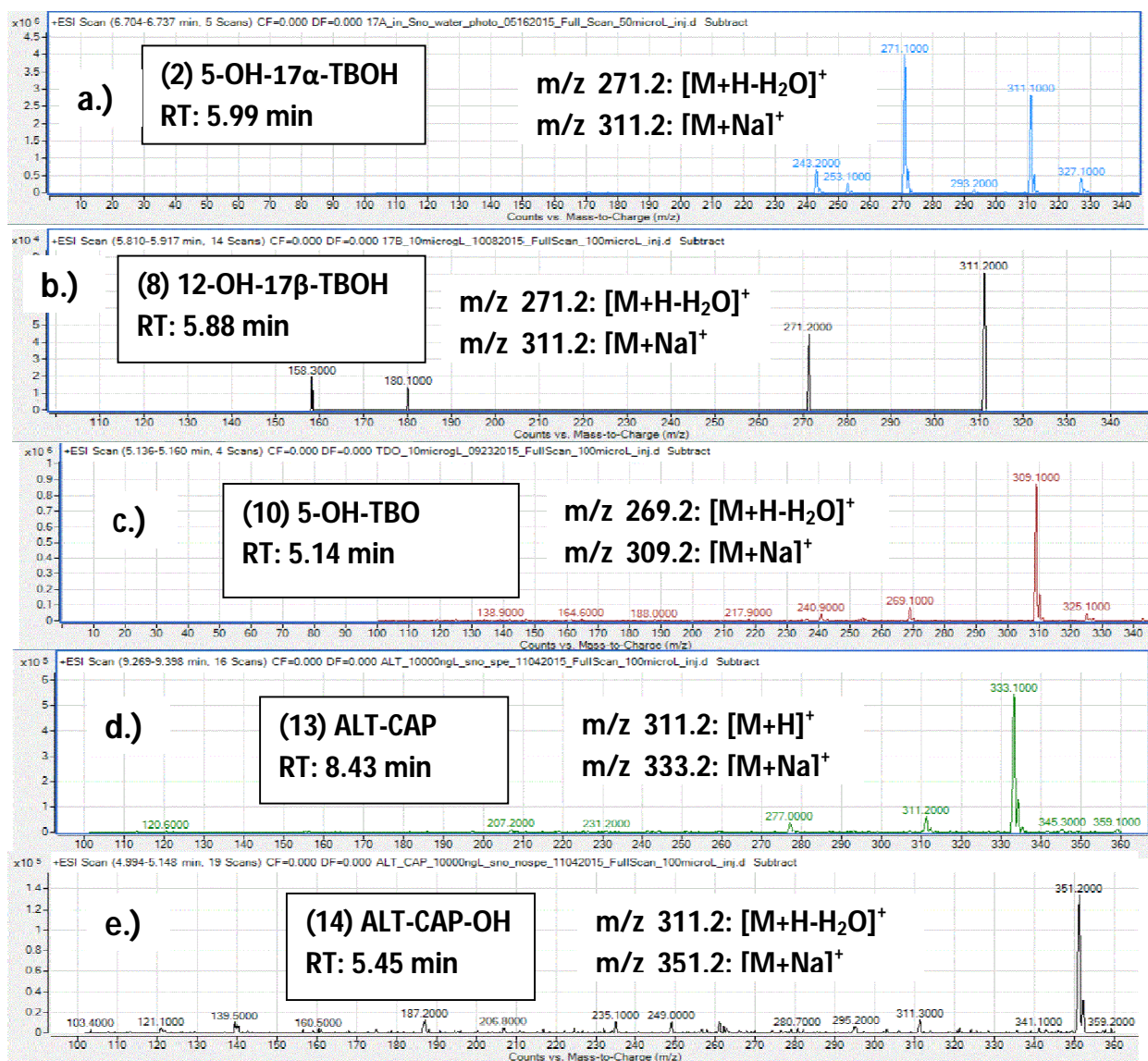
438 **Figure 7:** Chromatograms for a.) 17 β -TBOH, photo-reacted, solid phase extracted, b.) TBO,
 439 photo-reacted, solid phase extracted, c.) ALT, photo-reacted, acidified, solid phase extracted, and
 440 d.) ALT, photo-reacted, solid phase extracted. Includes prevalent ions and their retention times
 441 (RT), most common mass to charge ratios (m/z), and transition of each chromatogram. Figure 7a
 442 shows m/z 271.2->211.2, Figure 7b shows m/z 269.1->169.0, Figure 7c shows m/z 311.2-
 443 >227.0, and Figure 7d shows m/z 311.2->269.0.



444

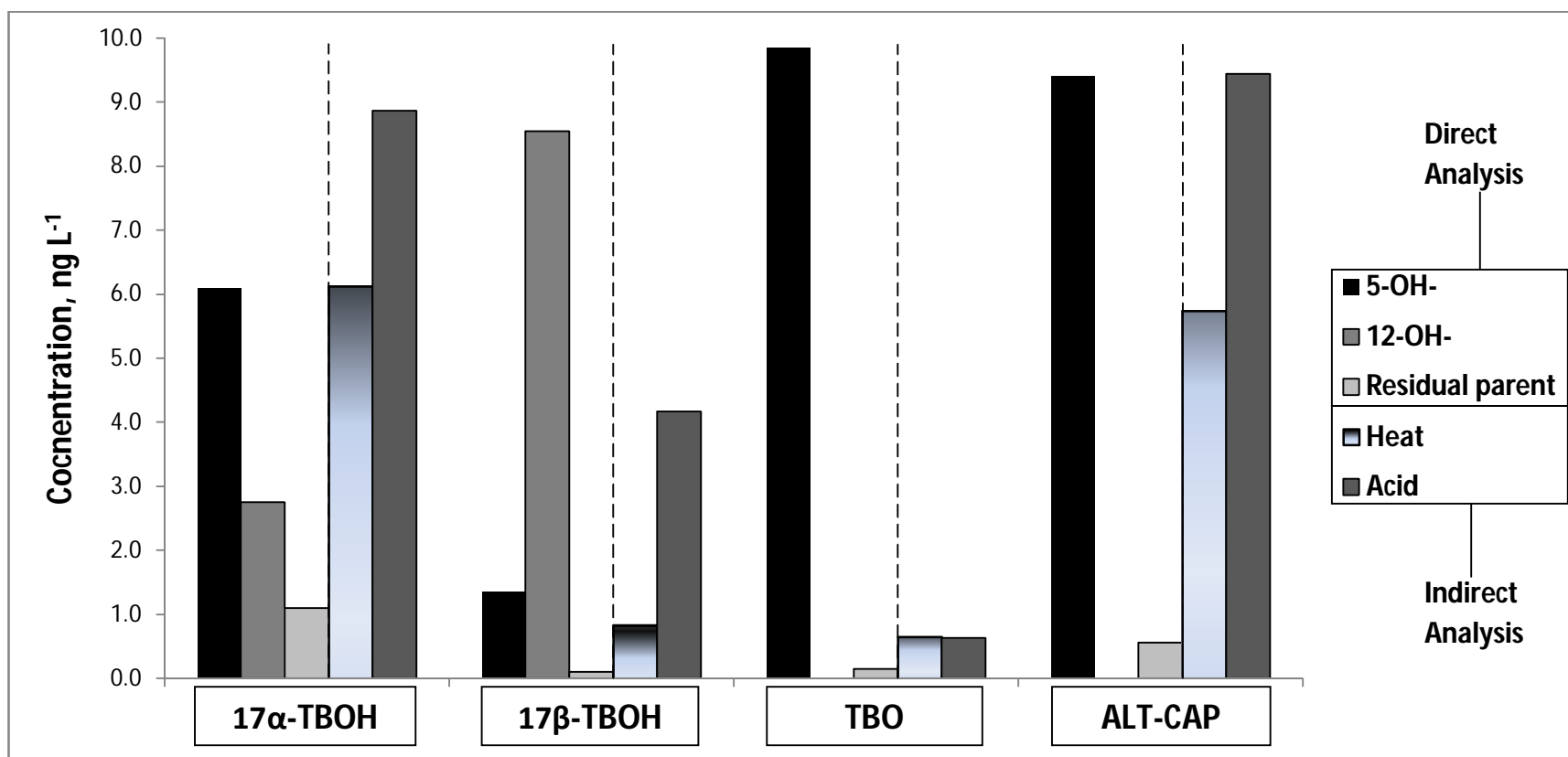
445

446 **Figure 8:** Spectra for a.) 17α -TBOH, b.) 17β -TBOH, c.) TBO, and d.) ALT, including retention
 447 time (RT) and most abundant mass-to-charge ratios (m/z) for each. Concentrations for each are
 448 10 ng/L. Figure 9a shows spectra representative of compounds (2), (3), and (4), and Figure 9b
 449 shows spectra representative of compounds (7) and (8).



450

451 **Figure 9:** Spectra for a.) 5-OH- 17α -TBOH, b.) 12-OH- 17β -TBOH, c.) 5-OH-TBO, d.) ALT-
 452 CAP, and e.) ALT-CAP-OH, including retention time (RT) and most abundant mass-to-charge
 453 ratios (m/z) for each. Concentrations for each are 10 ng/L.



454

455 **Figure 10:** Indirect photoproduct analysis via acidification or heat, for the primary photoproducts of trenbolone metabolites and ALT-
 456 CAP-OH. All concentrations are recovered from 10 ng L⁻¹ spikes. Acidified samples were adjusted to pH~2 using HCl after
 457 photoreaction. and heated samples were left in a 50° C water bath for 15 hours. 5-OH-, 12-OH- photoproducts and residual parent
 458 values are direct photoproduct measurements taken from samples photoreacted without purposeful reversion (left of dashed lines).
 459 Heat and acid results were the change in parent concentration after reversion (right of dashed lines).

460 **List of Tables**

461 **Table 1:** Elution times, Multiple reaction monitoring (MRM) transitions, fragmenter voltages, and collision energies for trenbolone
 462 metabolites, altrenogest, and photoproducts. MRM transitions, fragmenter voltages, and collision energies shown are quantitative
 463 (confirmatory) for each compound.

Compound	Retention time (min)	MRM Transitions (m/z)	Fragmenter (V)	Collision Energy (eV)
(1) 17 α -TBOH	7.55	271>253 (271>211)	135 (135)	30 (30)
(2) 5-OH-17 α -TBOH	6.62	271>211 (271>253)	135 (135)	30 (30)
(3) 12-OH-17 α -TBOH	7.13	271>211 (271>253)	135 (135)	30 (30)
(4) 5-OH-17 α -TBOH analog	6.93	271>211 (271>253)	135 (135)	30 (30)
(5) 17 α -TBOH analog	7.87	271>211 (271>253)	135 (135)	30 (30)
(6) 17 β -TBOH	7.23	271>253 (271>211)	135 (135)	30 (30)
(7) 5-OH-17 β -TBOH	4.87	271>211 (271>253)	135 (135)	30 (30)
(8) 12-OH-17 β -TBOH	5.85	271>211 (271>253)	135 (135)	30 (30)
(9) TBO	6.65	269>225 (269>169)	135 (135)	28 (28)
(10) 5-OH-TBO	5.14	269>169 (269>225)	135 (135)	28 (28)
(11) 17 α -d3-TBOH	7.58	274>256 (274>214)	135 (135)	30 (30)
(12) ALT	9.37	311>227 (311>269)	82 (82)	24 (12)
(13) ALT-CAP	8.41	311>269 (311>227)	82 (82)	12 (24)
(14) ALT-CAP-OH	5.43	311>269 (311>227)	82 (82)	12 (24)

464

465 **Table 2:** Method detection limits (MDL) and quantification limits (MQL), linear regression slopes, intercepts, coefficients of
 466 determination (R^2), matrix effects, recoveries from solid phase extraction, relative standard deviations (RSD) at high (10 ng L^{-1}) and
 467 low (1 ng L^{-1}) spikes, reversion from photoproducts to parent metabolites, and number of points used in regression, for trenbolone
 468 metabolites, altrenogest, and photoproducts. Responses of compounds (3), (4), (5), and (8) in lake water were below detection at tested
 469 levels, and were not pursued at higher concentrations since they are minor photoproducts or analogs.

470

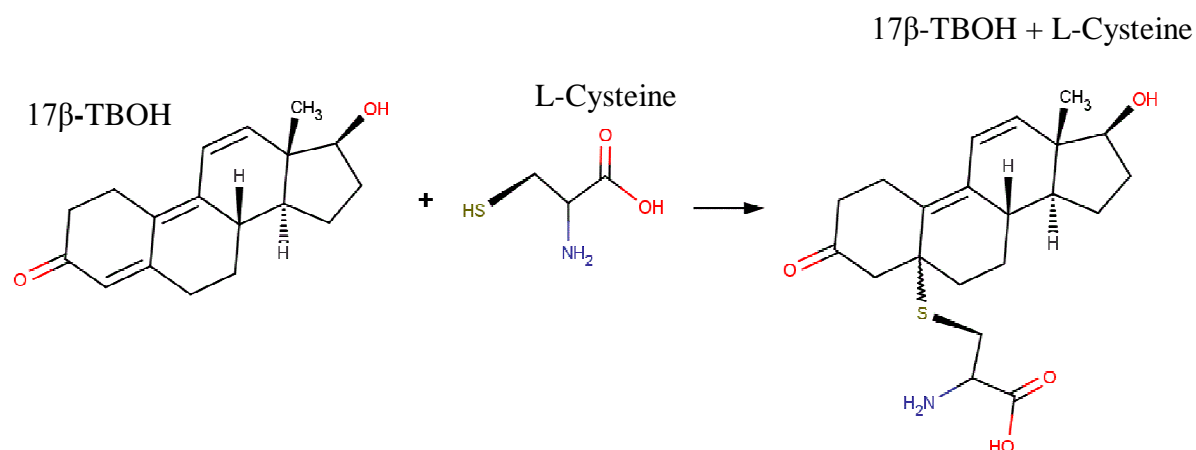
471

Compound	Solvent	MDL (ng/L)	MOQ (ng/L)	Slope	Intercept	R ²	Matrix Effect	Recovery	RSD (low spike)	RSD (high spike)	Reversion
(1) 17 α -TBOH	river water	0.03	0.04	0.075	-0.053	0.999	100%	115%	10%	14 %	N/A
	lake water	0.16	0.23	0.18	-0.32	0.996	84%	103%	39%	19%	N/A
(2) 5-OH-17 α -TBOH	river water	0.01	0.03	0.021	0.066	0.991	100%	104%	14%	12%	9%
	lake water	0.45	0.78	0.014	0.008	0.997	83%	107%	13%	11%	11%
(3) 12-OH-17 α -TBOH	river water	0.23	0.53	0.002	0.01	0.991	100%	125%	6%	4%	9%
(4) 5-OH-17 α -TBOH analog	river water	0.17	0.36	0.003	0.015	0.991	N/A	N/A	34%	22%	9%
(5) 17 α -TBOH analog	river water	0.61	1.19	0.001	-0.003	0.989	N/A	N/A	51%	48%	N/A
(6) 17 β -TBOH	river water	0.07	0.10	0.014	-0.011	0.999	100%	105%	13%	18%	N/A
	lake water	0.57	0.80	0.024	-0.159	0.998	85%	119%	26%	14%	N/A
(7) 12-OH-17 β -TBOH	river water	0.36	0.79	0.026	0.144	0.998	100%	81%	8%	13%	1%
	lake water	1.02	1.41	0.028	-0.019	0.999	88%	93%	17%	1%	9%
(8) 5-OH-17 β -TBOH	river water	1.51	3.63	0.004	-0.008	0.999	100%	75%	10%	26%	1%
(9) TBO	river water	0.05	0.07	0.051	-0.029	0.997	100%	115%	7%	14%	N/A
	lake water	0.26	0.30	0.106	-0.072	0.999	117%	107%	17%	23%	N/A
(10) 5-OH-TBO	river water	0.33	0.57	0.019	-0.359	0.996	100%	116%	26%	8%	11%
	lake water	0.59	0.94	0.047	0.401	0.998	108%	95%	15%	7%	10%
(12) ALT	river water	0.03	0.03	0.745	-1.71	0.997	100%	96%	4%	10%	N/A
	lake water	0.05	0.06	1.135	-2.132	0.996	74%	90%	15%	13%	N/A
(13) ALT-CAP	river water	0.03	0.03	0.407	-0.929	0.997	100%	104%	9%	3%	100%
	lake water	0.07	0.10	0.369	-0.717	0.997	79%	88%	3%	12%	100%
(14) ALT-CAP-OH	river water	0.08	0.09	0.06	0.027	0.991	100%	110%	10%	15%	30%
	lake water	0.34	0.44	0.105	-0.37	0.995	84%	99%	15%	21%	26%

474 Chapter 3: Thiol Adduct Formation

475 Introduction

476 Previous research at the University of Nevada, Reno discovered a potential adduct
477 between 17 β -TBOH and the amino acid L-cysteine during experiments to determine the rates of
478 anaerobic biodegradation trenbolone metabolites under anaerobic and anoxic conditions.
479 Observations of controls of 17 β -TBOH in microcosms reduced with L-cysteine indicated that the
480 17 β -TBOH would rapidly disappear. Subsequent tests via diode-array-detector HPLC strongly
481 suggested that 17 β -TBOH (peak absorbance 350 nm¹⁰) and L-cysteine (peak absorbance 250
482 nm³¹) formed a thiol adduct likely via Michael addition³² (see Figure 2).



484 **Figure 2:** Possible pathway for thiol-adduct formation between 17 β -TBOH and L-cysteine.

485 L-cysteine is a common amino acid, one of the building blocks of proteins, and many
486 anoxic or anaerobic environments contain similar compounds. Therefore in cattle treated with
487 trenbolone acetate, it is possible that trenbolone metabolites could form adducts with L-cysteine,
488 along with other compounds with free thiols (such as glutathione) in the animal gut or manure. If

489 this were the case, then MS/MS analysis, a common method for the detection of trenbolone
490 metabolites^{10,23,33}, would not easily detect an L-cysteine -- trenbolone adduct.

491 More importantly, there exist many examples of reversibility in thiol binding, suggesting
492 that adducts might represent metastable products subject to reversible reactions when water
493 quality conditions change. Like the reversible photochemical hydration-thermal dehydration
494 reactions, the possibility may exist of reversibility in systems with steroids and reduced sulfur. If
495 this were the case, then trenbolone metabolite conjugates could remain stable in anaerobic
496 systems (manure piles) for extended periods of time, then reverse and release trenbolone
497 metabolites into natural systems representing new transport pathways.

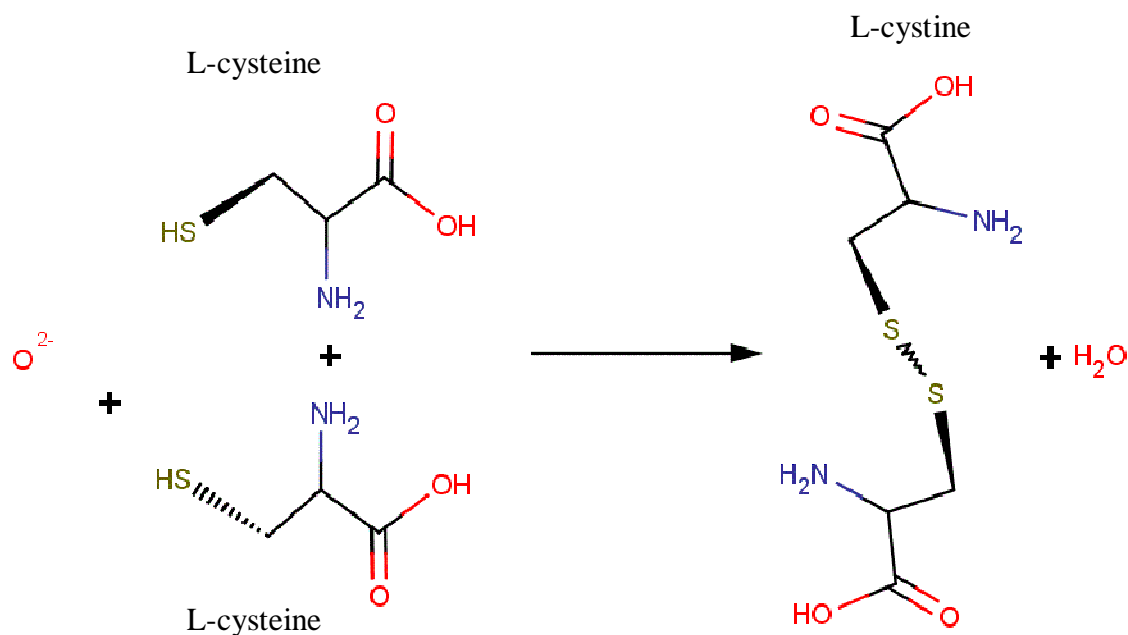
498 **Research Objective**

499 The critical research objective was to investigate whether thiol adducts between L-cysteine and
500 trenbolone are reversible upon changes in solution conditions, and if so, whether such changes
501 can occur at environmental conditions.

502 **Experimental**

503 Samples were processed in an anaerobic glove box (nitrogen filled) to minimize potential
504 oxidation of L-cysteine to L-cystine (see Figure 3). Inside the glove box, a single sample was
505 created comprised of an aqueous solution split into three 250 mL glass bottles, (each baked at
506 100° C for an hour prior to use). The solution was prepared in nitrogen-sparged water (NSW) by
507 adding approximately 246 mL of NSW to the bottle, adding 2.0 mL of a 2500 mg L⁻¹ methanolic
508 stock of 17β-TBOH to the solution, then adding L-cysteine-anhydride (89 mg) to the solution,
509 and adding 2 mL of 1 M aqueous NaOH solution to the bottle (20 mg L⁻¹ 17β-TBOH and 357 mg
510 L⁻¹ L-cysteine (40:1 L-cysteine:17β-TBOH)). Samples were reacted for 48 hours in the glove

511 box. Previous tests had shown that the half-life of the forward reaction was approximately 15
512 hours, and that the reaction reached equilibrium at 24-30 hours, with all available 17 β -TBOH
513 transforming to adducts.



514

515 Figure 3: L-cysteine oxidation to L-cystine in the presence of oxygen.

516 After the samples (250 ml) were allowed to react, they all were solid-phase extracted
517 onto a single C18 cartridge. Each cartridge was eluted with 9 mL of 95% methanol, 5% DDW,
518 dried down (completely) using a rotating evaporator, and then resuspended in methanol (2 mL).
519 The sample was then injected onto a preparation-scale HPLC to separate the parent compounds
520 from the adduct(s) (the products of the forward reaction). Peaks (including parents and products)
521 in the chromatogram were previously identified using HPLC-DAD (Agilent 1260, Agilent, Santa
522 Clara, California) and smaller samples, thus enabling accurate isolation of larger quantities of

523 product on the prep-scale HPLC. Prep-scale HPLC conditions were 50 mL min⁻¹ flow rate, C18
524 column, solvents were A: DDW with 0.1% acetic acid, and B: Acetonitrile (ACN) with 0.1%
525 acetic acid. Separation was accomplished with the following gradient: 25% B initially, increased
526 to 72% over 18 min, increased to 100% B over 0.01 min, isocratic at 100% B for 1 min,
527 decreased to 25% over 0.01 min, isocratic at 25% B for 6 min, for a total runtime of 25 min³⁰.

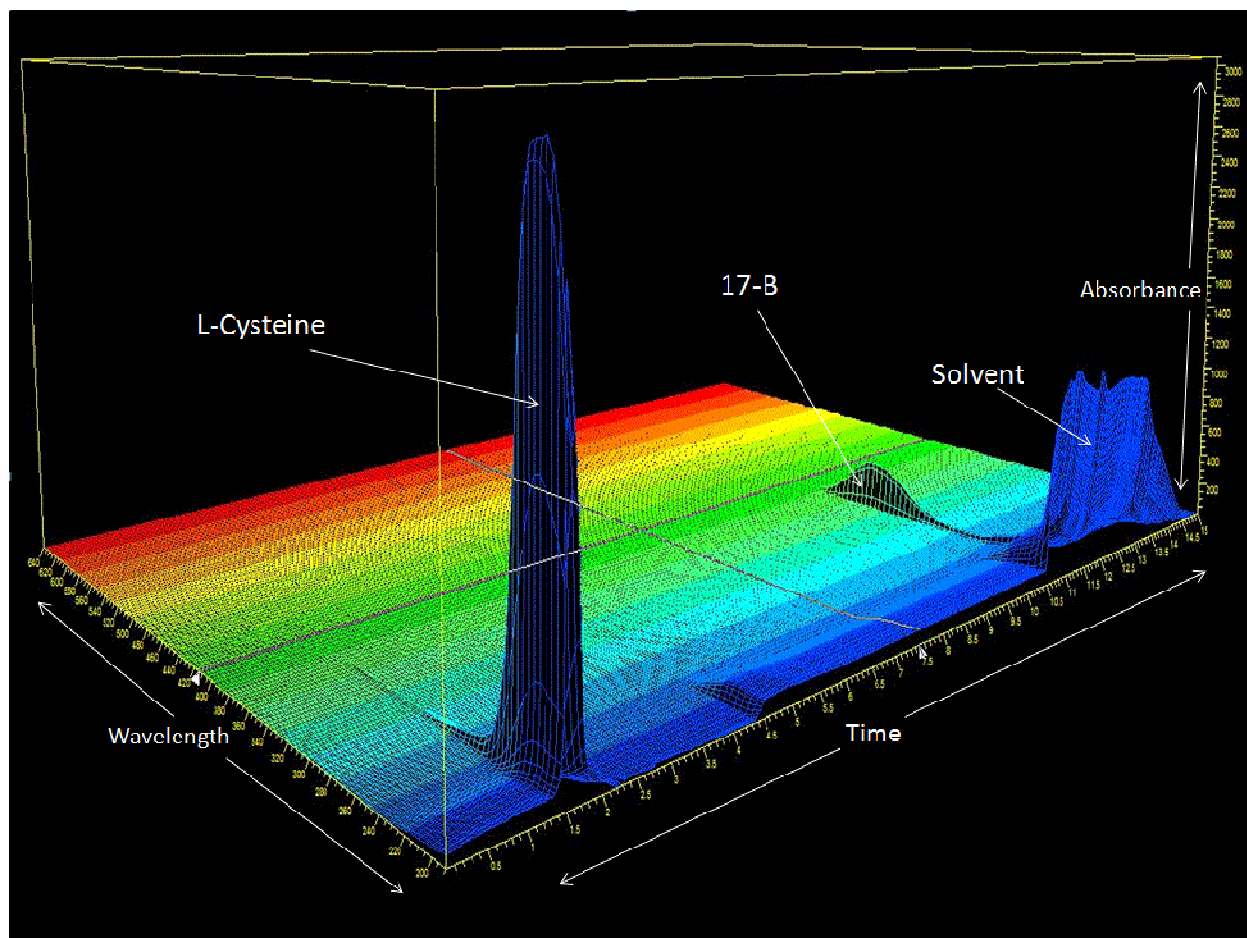
528 **Deaerating Water**

529 To optimize the stoichiometry of L-cysteine - trenbolone adduct formation, steps were
530 taken to deaerate water to reduce the oxidative-reductive potential of the system and the mass of
531 L-cysteine required. Titanium (III) citrate was produced according to Jones and Pickard³⁵, and
532 added to NSW prior to L-cysteine and trenbolone addition to reduce the amount of L-cysteine
533 required to form adducts. However, the use of this deaerated water resulted in the formation of
534 titanium oxides which clogged SPE cartridges, preventing sample analysis. It is recommended
535 that another reducing agent be used for further efforts (keeping in mind that any reducing agent
536 with an active thiol group on it (dithiothreitol, glutathione, etc.) will theoretically react with
537 trenbolone just as L-cysteine does.

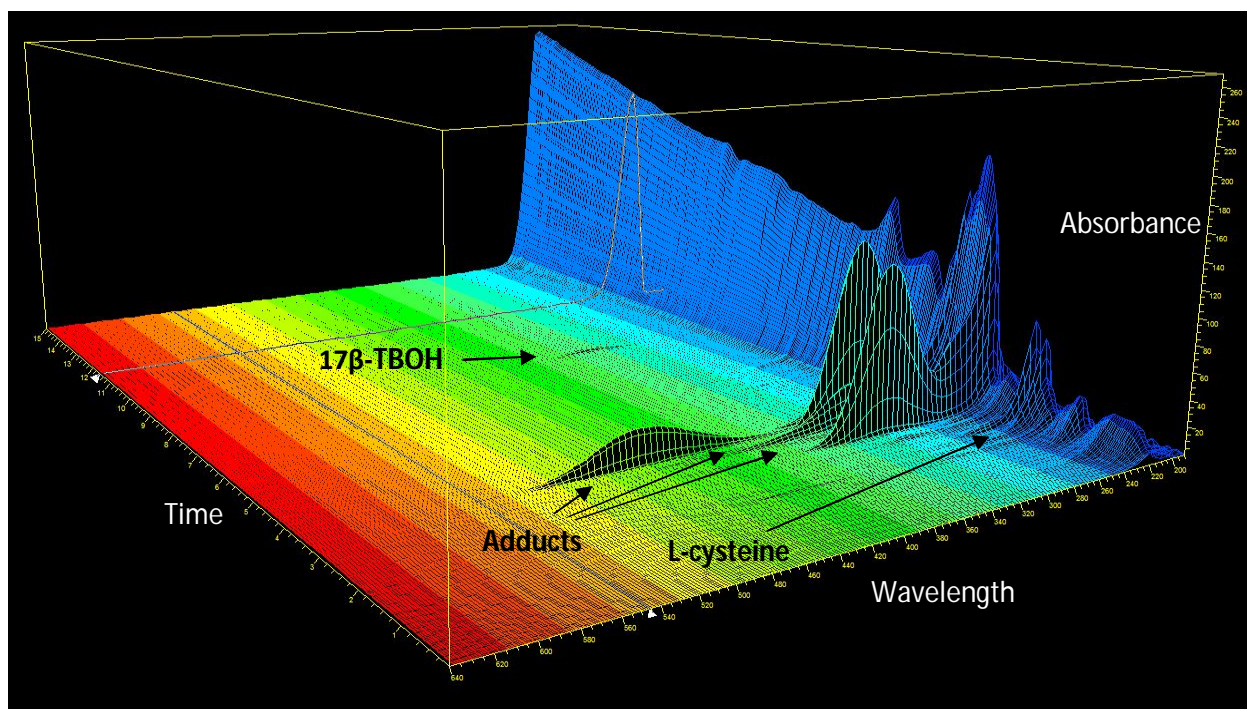
538 **Adduct Formation**

539 L-cysteine and 17 β -TBOH were detected via HPLC-DAD (see figure 4). When a molar
540 excess of L-cysteine was present, 17 β -TBOH-L-cysteine adducts formed (see figure 5). After the
541 adduct was formed, efforts were made to isolate it for NMR analysis, and adduct reversibility
542 was investigated as a function of changing solution conditions. Samples were fraction collected
543 as described above, and either lyophilized (freeze-dried via submersion in liquid nitrogen, then
544 placed under vacuum) or dried down under vacuum at room temperature. Samples were then re-

545 suspended in deuterated solvents for NMR analysis (University of Nevada, Reno, Chemistry
546 department). Due to interference from residual water, analysis could not determine conclusively
547 any adduct structures.



548
549 Figure 4: 3-dimensional chromatogram showing L-cysteine (retention time ~2 min, peak
550 absorbance 220 nm) and 17 β -TBOH (retention time ~11.5 min, peak absorbance 346 nm),
551 measured via HPLC-DAD, prior to reaction.



552

553 Figure 5: 3-dimensional chromatogram showing 17 β -TBOH-L-cysteine adducts (at ~3-3.5 min),
 554 with some residual 17 β -TBOH and L-cysteine after reaction. Note the "wall" of background
 555 signal at low wavelengths (~200 nm).

556 Adduct Stability

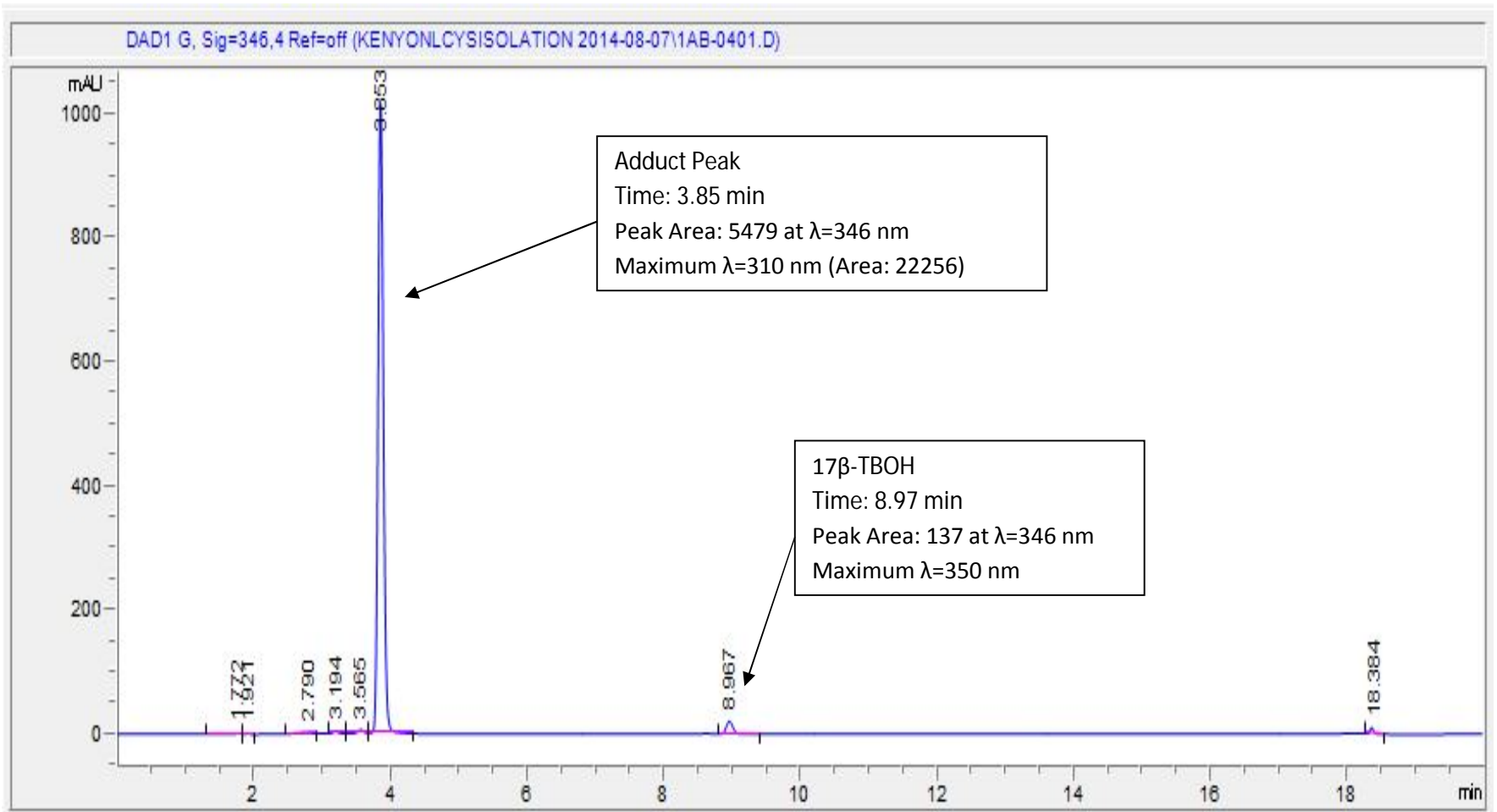
557 To explore whether adduct reversibility could regenerate trenbolone, solution conditions
 558 were changed in adduct samples post fractionation. After fraction collection, two vials (totaling
 559 approximately 30 mL of solution) of product were isolated from the prep-scale HPLC, and split
 560 into a total of eleven 2 mL samples for testing. Two of these samples were controls (pH
 561 measured was 4). Three samples were heated at 80 $^{\circ}$ C for 2 hours using a water bath and
 562 mercury thermometer. Three samples were pH-adjusted to pH 13 using 1 M NaOH, and three
 563 samples were adjusted to pH 13 and subsequently heated for 2 hours at 80 $^{\circ}$ C in a water bath.

564 Neither aerobic conditions alone, nor combined with heating or alkaline conditions
565 altered adduct stability (see Figures 6-8), but aerobic, alkaline conditions with subsequent
566 heating did regenerate 17 β -TBOH (see Figure 9). However, analysis of peak areas showed that
567 while a decrease in adduct peak did occur, it did not decrease proportionally to the amount of
568 17 β -TBOH which reappeared, suggesting insufficient analytical sensitivity or an unidentified
569 source of complexed 17 β -TBOH. It is also possible that 17 β -TBOH has a lesser peak area
570 response factor in UV-DAD than its adduct with L-cysteine, such that the small difference in the
571 adduct peak could correspond to the increase in 17 β -TBOH.

572 **Conclusions**

573 Regarding the first research objective (a single method to detect all metabolites and
574 photoproducts of trenbolone acetate, as well as altrenogest and its photoproducts), a method was
575 successfully developed. With separation, simultaneous detection is possible, however due to
576 coelution between metabolites and photoproducts of 17 α -TBOH and 17 β -TBOH in fast
577 chromatography runs (<20 min), accurate quantification in mixed residue systems can be
578 compromised. Fortunately, 17 α -TBOH is typically the dominant metabolite present, and thus
579 17 β -TBOH, TBO, and related photoproducts would usually be expected to occur at lower
580 concentrations as compared with 17 α -TBOH.

581 With regard to the second research objective, efforts to test the reversibility of 17 β -
582 TBOH-L-cysteine adducts yielded some insights into adduct stability. Future efforts maintaining
583 cysteine stability in solution, include improving analytical methods to observe adducts and more
584 comprehensive reversibility characteristics. Also, the fraction-collection and subsequent NMR
585 analysis of adducts to determine their structure would help to understand this system.

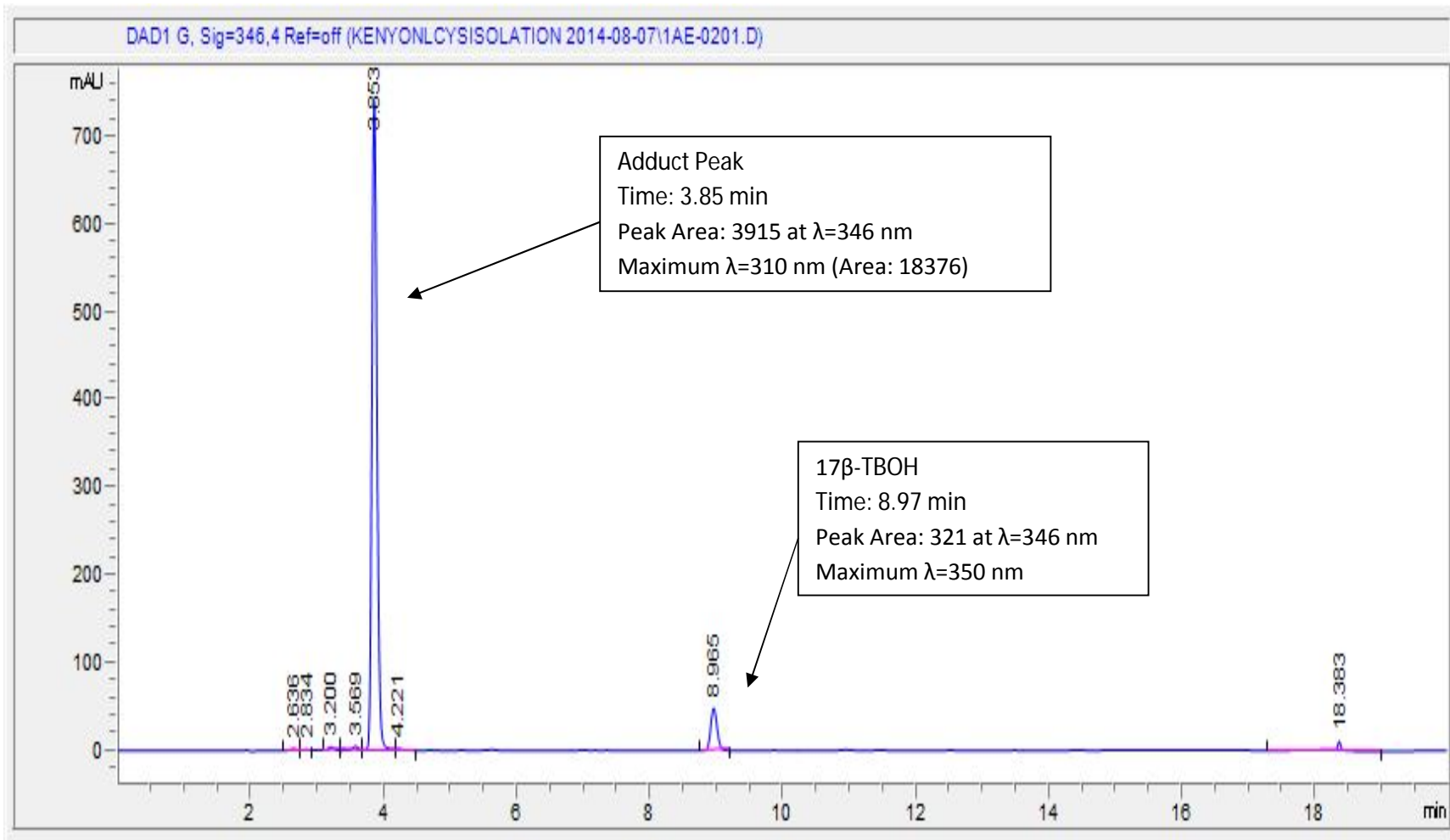


586

587 Figure 6: Fraction-collected L-cysteine-17β-TBOH adduct, control (pH=4).

588

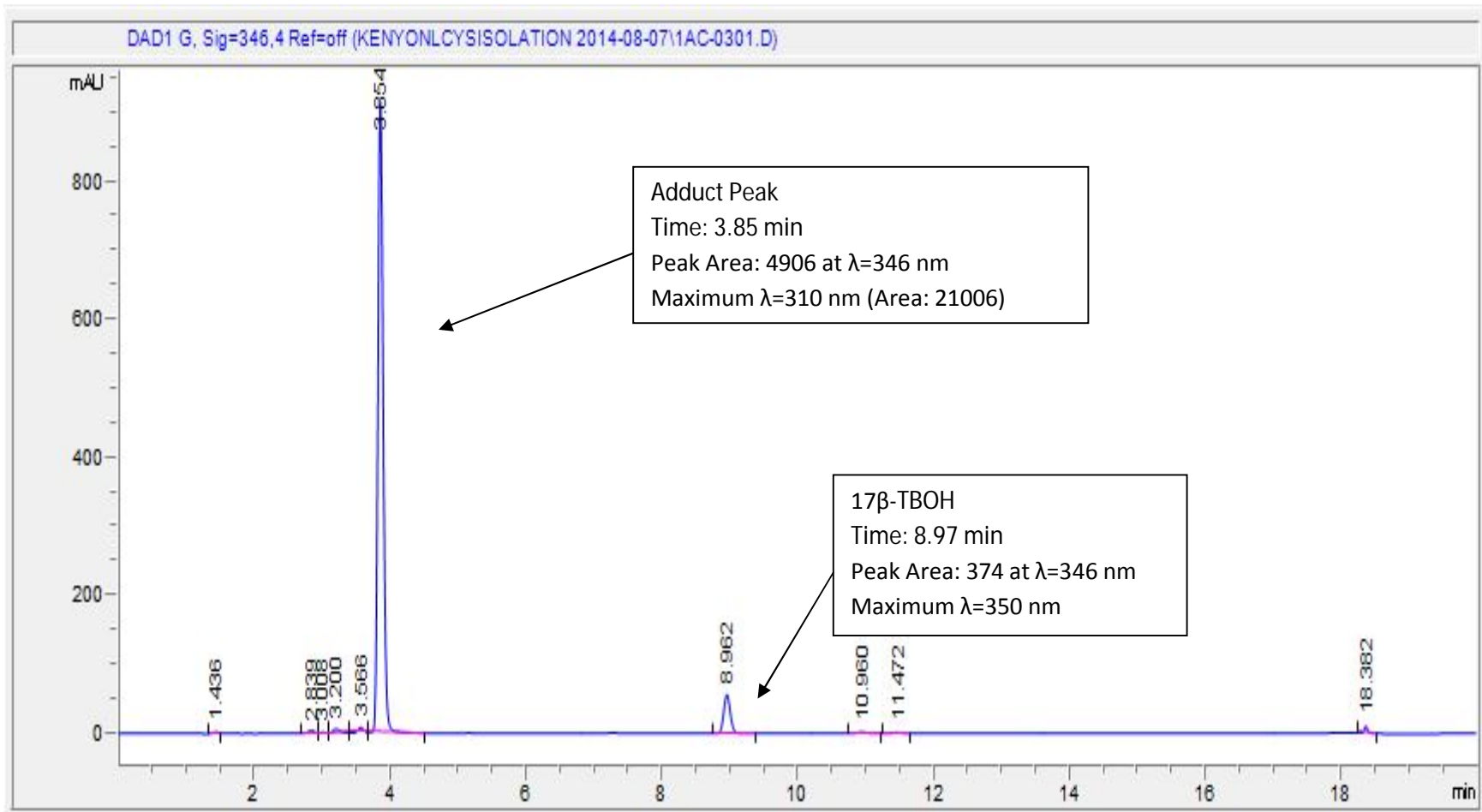
589



590

591 Figure 7: Fraction-collected L-cysteine-17 β -TBOH adduct, heated (80° C water bath for 2 hours) (pH=4).

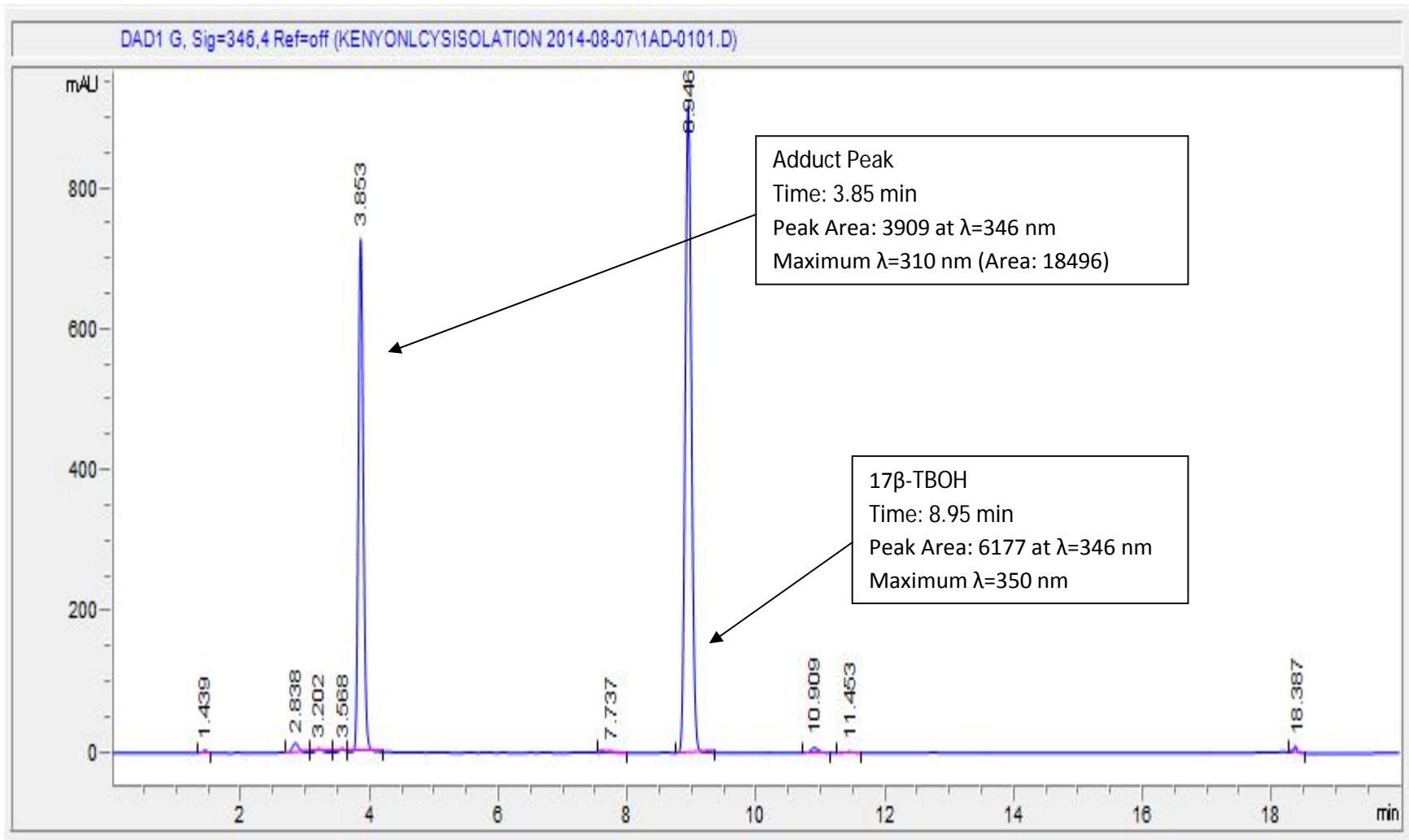
592



593

594 Figure 8: Fraction-collected L-cysteine-17 β -TBOH adduct, under alkaline (pH=13) conditions.

595



596

597 Figure 9: Fraction-collected L-cysteine-17 β -TBOH adduct, under alkaline (pH=13) conditions, then heated (80° C water bath for 2

598 hours) .

599 **Works Cited**

- 600 (1) Endocrine Disruptors. National Institute of Environmental Health Services. August 11,
601 2015. <http://www.niehs.nih.gov/health/topics/agents/endocrine/>
- 602 (2) Contaminants of Emerging Concern. United States Environmental Protection Agency.
603 May 8, 2014. <http://water.epa.gov/scitech/cec/>
- 604 (3) Sone, K.; M. H.; Itamoto, M.; Katsu, Y.; Watanabe, H.; Urushitani, H.; Tooi, O.;
605 Guillette Jr., L. J.; Taisen, I. Effects of an androgenic growth promoter 17 β trenbolone on
606 masculinization of Mosquitofish (*Gambusia affinis affinis*). *Gen. Comp. Endocrinol.* (2005) 143,
607 151–160.
- 608 (4) Jensen, K. M.; E. A. M.; Kahl, M. D.; Ankley, G. T. Effects of the Feedlot Contaminant
609 17 α Trenbolone on Reproductive Endocrinology of the Fathead Minnow. *Environ. Sci. Technol.*
610 (2006) 40, 3112-3117.
- 611 (5) Seki, M., S. Fujishima, T. Nozaka, M. Maeda & K. Kobayashi. Comparison of response
612 to 17 beta estradiol and 17 beta trenbolone among three small fish species. *Environ. Toxicol.*
613 *Chem.* (2006) 25, 2742-2752.
- 614 (6) Morthorst, J.E.; Holbech, H.; Bjerregaard, P. Trenbolone causes irreversible
615 masculinization of zebrafish at environmentally relevant concentrations. *Aquat. Toxicol.* (2010).
616 98(4), 336-343.
- 617 (7) Orlando, E. F.; Kolok, A. S.; Binzcik, G. A.; Gates, J. L.; Horton, M. K.; Lambright, C.
618 S.; Gray, L. E.; Soto, A. M.; Guillette, L. J. Endocrine-disrupting effects of cattle feedlot effluent
619 on an aquatic sentinel species, the fathead minnow. *Environ. Health Perspect.* (2004). 112(3),
620 353-258.
- 621 (8) Khan, B.; Lee, L. S., Estrogens and synthetic androgens in manure slurry from trenbolone
622 acetate/estradiol implanted cattle and in waste receiving lagoons used for irrigation.
623 *Chemosphere* (2012), 89, 1443-1449.
- 624 (9) Pottier, J.; Cousty, C.; Heitzman, R. J.; Reynolds, I. P. Differences in the
625 biotransformation of 17-beta-hydroxylated steroid, trenbolone acetate, in rat and cow.
626 *Xenobiotica.* (1981), 11(7), 489-500.
- 627 (10) Khan, B.; Lee, L. S.; Sassman, S. A. Degradation of Synthetic Androgens 17 α and 17 β
628 Trenbolone and Trendione in Agricultural Soils. *Environ. Sci. Technol.* (2008), 42, 3570-3574.
- 629 (11) Lange, I. G.; Daxenberger, A.; Schiffer, B.; Witters, H.; Ibarreta, D.; Meyer, H. H. D. Sex
630 hormones originating from different livestock production systems: fate and potential disrupting
631 activity in the environment. *Analytica Chimica Acta.* (2002). 473, 27-37.

- 632 (12) Steroid Hormones. The Merck Veterinary Manual. December 2013.
633 http://www.merckvetmanual.com/mvm/pharmacology/growth_promotants_and_production_enhancers/steroid_hormones.html
634
- 635 (13) Wammer, K. H.; Anderson, K. C.; Erickson, P. R.; Kliegman, S.; Moffatt, M.; Berg, S.
636 M.; Heitzman, J. A.; McNeill, K.; Martinovic-Weigelt, D.; Cwiertny, D. M.; Kolodziej, E. P.
637 Environmental photochemistry of altrenogest: photoisomerization to a bioactive product with
638 increased environmental persistence via reversible photohydration. In review.
- 639 (14) Squires, E.L.; Heesemann, C.P.; Webel, S.K.; Shideler, R.K.; Voss, J.L. Relationship of
640 altrenogest to ovarian activity, hormone concentrations and fertility of mares. *J. Anim. Sci.*
641 (1983). 56, 901-910.
- 642 (15) van Leeuwen, J.J.J.; Williams, S.I.; Martens, M.R.T.M.; Jourquin, J.; Driancourt, M.A.;
643 Kemp, B.; Soede, N.M. The effect of post weaning altrenogest treatments of primiparous sows
644 on follicular development, pregnancy rates, and litter sizes. *J. Anim. Sci.* (2011). 89, 397-403.
- 645 (16) Willmann, C.; Schuler, G.; Hoffmann, B.; Parvizi, N.; Aurich, C. Effects of age and
646 altrenogest treatment on conceptus development and secretion of LH, progesterone, and eCG in
647 early-pregnant mares. *Theriogenology* (2011). 75, 421-428.
- 648 (17) Regu-Mate® Product label. Regu-Mate®. 2010. <http://www.regu-mate.com/label.asp>
- 649 (18) Estienne, M.J.; Harper, A.F.; Horsley, B.R.; Estienne, C.E.; Knight, J.W. Effects of P.G.
650 600 on the onset of estrus and ovulation rate in gilts treated with Regu-mate. *J. Anim. Sci.*
651 (2001). 79, 2757-2761.
- 652 (19) Zeilinger, J.; Steger-Hartmann, T.; Maser, E.; Goller, S.; Vonk, R.; Lange, R. Effects of
653 synthetic gestagens on fish reproduction. *Environ. Tox. Chem.* (2009). 28(12), 2663-2670.
- 654 (20) Säfholm, M.; Ribbenstedt, A.; Fick, J.; Berg, C. Risks of hormonally active
655 pharmaceuticals to amphibians: a growing concern regarding progestagens. *Philos. T. Roy. Soc.*
656 *A.* (2014). 369, 20130577.
- 657 (21) Kumar, V.; Johnson, A.C.; Trubiroha, A.; Tumova, J.; Ihara, M.; Grabic, R.; Kloas, W.;
658 Tanaka, H.; Kroupova, H.K. The challenge presented by progestins in ecotoxicological research:
659 A critical review. *Environ. Sci. Technol.* (2015). 49, 2625-2638.
- 660 (22) Jones, G. D.; Benchetler, P. V.; Tate, K. W.; Kolodziej, E. P. Trenbolone acetate
661 metabolite transport in rangelands and irrigated pasture: observations and conceptual approaches
662 for agro-ecosystems. *Environ. Sci. Technol.* (2014). 48(21), 12569-12576.
- 663 (23) Durhan, E. J.; Lambright, C. S.; Makynen, E. A.; Lazorchak, J.; Hartig, P. C.; Wilson, V.
664 S.; Gray, L. E.; Ankley, G. T. Identification of metabolites of trenbolone acetate in androgenic
665 runoff from a beef feedlot. *Environ. Health Perspect.* (2006), 114, 65-68.

- 666 (24) Cole, E. A.; McBride, S. A.; Kimbrough, K. C.; Lee, J.; Marchand, E. A.; Cwiertny, D.
667 M.; Kolodziej, E. P. Rates and product identification for trenbolone acetate metabolite
668 biotransformation under aerobic conditions. *Environ. Tox. Chem.* (2015). *34*(7), 1472-1484.
- 669 (25) Schiffer, B.; Daxenberger, A.; Meyer, K.; Meyer, H. H. D., The Fate of Trenbolone
670 Acetate and Melengestrol Acetate after Application as Growth Promoters in Cattle:
671 Environmental Studies. *Environ. Health Perspect.* (2001). *109*, 7.
- 672 (26) Khan, B.; Qiao, X. L.; Lee, L. S. Stereoselective sorption by agricultural soils and liquid-
673 liquid partitioning of trenbolone (17 alpha nad 17 beta) and trendione. *Environ. Sci. Technol.*
674 (2009). *43*(23), 8827-8833.
- 675 (27) Card, M. L.; Chin, Y.-P.; Lee, L. S.; Khan, B. Prediction and experimental evaluation of
676 soil sorption by natural hormones and hormone mimics. *J. Agric. Food Chem.* (2012), *60*,
677 1480-1487.
- 678 (28) Altrenogest. Properties-Predicted-EpiSuite. Chemspider. 2015.
679 [http://www.chemspider.com/Chemical-Structure.8216634.html?rid=da4d7a65-097e-41b2-8b82-](http://www.chemspider.com/Chemical-Structure.8216634.html?rid=da4d7a65-097e-41b2-8b82-649f22b8295a)
680 [649f22b8295a](http://www.chemspider.com/Chemical-Structure.8216634.html?rid=da4d7a65-097e-41b2-8b82-649f22b8295a)
- 681 (29) Qu, S.; Kolodziej, E. P.; Cwiertny, D. M., Phototransformation Rates and Mechanisms
682 for Synthetic Hormone Growth Promoters Used in Animal Agriculture. *Environ. Sci. Technol.*
683 (2012), *46*, 13202-13211.
- 684 (30) Kolodziej, E. P.; Qu, S.; Forsgren, K. L.; Long, S. A.; Gloer, J. B.; Jones, G. D.; Schlenk,
685 D.; Baltrusaitis, J.; Cwiertny, D. M. Identification and Environmental Implications of Photo
686 Transformation Products of Trenbolone Acetate Metabolites. *Environ. Sci. Technol.* (2013), *47*,
687 5031-5041.
- 688 (31) Forsgren, K. L.; Qu, S.; Lavado, R.; Cwiertny, D.; Schlenk, D. Trenbolone acetate
689 metabolites promote ovarian growth and development in adult Japanese medaka (*Oryzias*
690 *Latipes*). *Gen. Comp. Endocrinol.* (2014), *202*, 1-7.
- 691 (32) Avi-Dor, Y.; Mager, J. A spectrophotometric method for determination of cysteine and
692 related compounds. *J. Biol. Chem.* (1956). *222*, 249-258.
- 693 (33) Nair, D. P.; Podgorski, M.; Chatani, S.; Gong, T.; Xi, W.; Fenoli, C. R.; Bowman, C. N.
694 The thiol-Michael addition click reaction: a powerful and widely used tool in materials
695 chemistry.
- 696 (34) Webster, J. P.; Kover, S. C.; Bryson, R. J.; Harter, T.; Mansell, D. S.; Sedlak, D. L.;
697 Kolodziej, E. P. Occurrence of Trenbolone Acetate Metabolites in Simulated Confined Animal
698 Feeding Operation (CAFO) Runoff. *Environ. Sci. Technol.* (2012), *46*, 3803-3810.
- 699 (35) Jones, G. A.; Pickard, M. D. Effect of titanium (III) citrate as reducing agent on growth
700 of rumen bacteria. *Appl. Environ. Microbiol.* (1980). *39*(6), 1144-1147.